The Thesis Committee for Asha Tarika Fleury
Certifies that this is the approved version of the following thesis:

Degradable poly(ethylene glycol) based hydrogels for pulmonary drug delivery and *in vitro* T cell differentiation applications

APPROVED BY
SUPERVISING COMMITTEE:

Supervisor:

Krishnendu Roy

Laura Suggs

Degradable poly(ethylene glycol) based hydrogels for pulmonary drug delivery and *in vitro* T cell differentiation applications

by

Asha Tarika Fleury, B.S.

Thesis

Presented to the Faculty of the Graduate School of

The University of Texas at Austin

in Partial Fulfillment

of the Requirements

for the Degree of

Master of Science in Engineering

The University of Texas at Austin

August 2013

Dedication

This work is dedicated to my family for their endless love, guidance, and encouragement. To John Peter, Jamuna, Anjali, and Kesari, I love you all so much for being my support system and for being my closest friends. Thank you for staying by my side and inspiring me to be the best person I can be, intellectually and spiritually.

Acknowledgements

First and foremost, I would like to thank Dr. Krishnendu Roy for being my advisor and teacher for all these years. I feel fortunate to have such a great mentor who was willing to give me an opportunity to conduct research in his laboratory. His guidance and encouragement were critical to my development as a better researcher and a better person. I would also like to thank Dr. Laura Suggs for being my second reader on this thesis and for her invaluable input and feedback. Thank you to Dr. Nicholas Peppas for his guidance since I entered the department as an undergraduate in 2006 and for giving me my first research position in his lab.

I would like to express my gratitude to the many research staff members at the University of Texas at Austin that have assisted me. Dr. Alan Watts and Dr. Greg Lyness at TherapUTex greatly assisted me with NGI experiments and provided crucial advice and input on pulmonary formulations for this project. Also, Dr. Irina Fernandez assisted many hours with FACS analysis, cell sorting, and interpretation of my data. Dwight Romanovicz assisted on SEM and all the staff at the Animal Resources Center assisted with animal studies. I would also like to thank all the faculty and staff in the Department of Biomedical Engineering at the University of Texas at Austin. I am grateful to have been part of this amazing department.

I am especially thankful towards all the Roy lab members for being supportive colleagues and good friends. Special thanks to labmate Prinda Wanakule for starting the pulmonary microgel project, mentoring me in the lab, and being my first friend in graduate school. I would also like to thank Anuj Kudva for willingly assisted me for countless hours without complaint and offered invaluable input on my research. Also, I

am grateful towards Myung Hee Michelle Kim and Tracy Ooi for all their help in the T cell project and endless patience in training me in the lab. The rest of the Roy lab members, Eileen Dawson, Jardin Leleux, Rachit Agarwal, Pallab Pradhan, Naveen Mehta, Gary Liu, and Michelle Miller have provided so much support and help throughout the past two years that have made this thesis possible. I have enjoyed being a part of "Klub Krish" and value the experiences and relationships I have gained.

Finally, I would like to extend my deepest gratitude to my family that has supported me throughout my studies. I especially want to thank my parents, John Peter and Jamuna, for providing me with limitless love and inspiration. My beloved sisters, Anjali and Kesari, are my role models and best friends and are always encouraging me to work my hardest. I would also like to thank Hyung Harideva, Mina, Jivan, Prakash, and Jyoti Luu for always being a supportive family for me and my dear friends. Also, thanks to my grandparents for giving me strength, love, and encouragement to reach my goals.

Abstract

Degradable poly(ethylene glycol) based hydrogels for pulmonary drug delivery and *in vitro* T cell differentiation applications

Asha Tarika Fleury, M.S.E.

The University of Texas at Austin, 2013

Supervisor: Krishnendu Roy

Hydrogels, defined as three-dimensional, hydrophilic networks, offer extensive biomedical applications. The areas of application are heavily concentrated in drug delivery and tissue engineering because of the hydrogels' ability to mimic extracellular matrixes of tissue while maintaining a high level of biocompatibility. Specifically, poly(ethylene glycol) (PEG) is a well-established biomaterial in hydrogel applications due to its high water-solubility, low toxicity, high biocompatibility, and stealth properties.

This thesis discusses two applications of PEG-based degradable hydrogels. The first is the targeted, site-specific, controlled release of biologic drugs administered by inhalation. There are many challenges to designing a pulmonary delivery system for inhalation of biologic drugs such as low respirable fractions and short resident time in the lungs. In this report, the hydrogel microcarriers for encapsulated drugs were formed by cross-linked PEG and peptide sequences synthesized during a mild emulsion process. The microgels underwent freeze-drying in the presence of cryoprotectants and formulated for

dry powder inhalation. The microgels displayed swelling properties to avoid local macrophage clearance in the lungs and exhibited triggered release and degradation in response to enzyme for disease specific release. Dry formulations were tested for aerosolization properties and indicated ability to be delivered to the deep lung by a dry powder inhaler. Lastly, microgels were successfully delivered to mice lungs via intratracheal aerosol delivery.

This thesis also discusses the use of PEG-based hydrogel as a biomaterial microenvironment for encapsulated stem cells as a means of in vitro T cell differentiation. A 3D hydrogel system creates a biomimetic reconstruction of the cell's natural microenvironment and allows us to adjust factors such as ligand density and mechanical properties of the hydrogel in order to promote cells differentiation. This report utilizes hydrogels of cross-linked hyaluronic acid and PEG to encapsulate mice bone marrow hematopoietic progenitor cells in the presence of notch ligands, displayed through stromal cells, magnetic microbeads, or immobilized within the hydrogel matrix. Mechanical properties of the hydrogels were tested and the release of encapsulated cells was performed by enzymatic degradation or dissolution. The differentiation data obtained indicated successful differentiation of stem cells into early T cells through the hydrogel system.

Table of Contents

List of Tables

List of Figures

Chapter 1: Introduction and Overview

1.1 INTRODUCTION

The first synthetic hydrogel created by Wichterle and Lim in 1954 opened the doors for numerous medical applications, from tissue engineering to pharmaceutical formulations. The areas of application are heavily concentrated in drug delivery and tissue engineering applications due to the hydrogels' ability to mimic many roles of extracellular matrixes found in tissues while maintaining a high level of biocompatability. Hydrogels are hydrophilic, three-dimensional (3D) polymer networks capable of absorbing large quantities of water [1]–[4]. Various types of polymers have been studied and utilized to date. Recently, many advances have been made in the development of these crosslinked biomaterials, from their use as 3D polymer scaffolds that act as analogues to the natural extracellular matrices to their use as drug carrier systems for large molecular weight protein-based drugs in site-specific delivery [3], [4]. Using 3D hydrogels to encapsulate cells, proteins, ligands, and more allows us to create more biomimetic reconstructions of the cell's natural surrounding within tissue. It also gives us the tools to fine tune factors such as cell density, ligand density, and mechanical properties of the hydrogel in order to promote cell growth and differentiation in the case of stem cells. In terms of drug delivery, hydrogels offer the potential for targeted, site-specific, controlled release of therapeutic agents.

There are many design criteria that must be understood to create functional hydrogel systems specific for each application. One of the most significant functions of hydrogel systems is controlled degradation. Controlled degradation is critical in tissue engineering and drug delivery. Degradation of hydrogels typically occurs as a result of

hydrolysis, the action of enzymes, and/or dissolution [4]. This report utilizes degradable hydrogel systems to achieve disease-specific drug release due to enzymatic stimulus and to release encapsulated cells that undergo *in vitro* T cell differentiation within the tissue-mimicking hydrogel environment.

1.2 POLY(ETHYLENE GLYCOL)-BASED DEGRADABLE HYDROGEL SYSTEMS

Poly(ethylene glycol) (PEG) is a well-established biomaterial in hydrogel applications. It has been utilized as polymer-based protective drug carrier for targeted drug delivery, a covalently-attached biocompatible shield for stealth properties, and as a scaffold and microenvironment for encapsulated cells. PEG is considered non-toxic and resists recognition by the immune system. Its widespread use can be attributed to its biocompatible, non-immunogenic, non-antigenic, and hydrophilic properties. The polymer is FDA approved and used for many commercial products including Vigilon™ as a sheet wound covering material and Hypol™ as a foam for wound healing and drug delivery [3], [5]–[7].

PEG is available in a number of functionalized forms, including multi-armed and acrylated PEG. Acrylated PEG is especially useful in the crosslinking of hydrogels via conjugate addition and Michael addition reactions [7]–[9]. These reactions can be used in the presence of biologic active drugs for drug delivery purposes as well as in the presence of cells being encapsulated within hydrogels.

1.3 OVERVIEW

Chapter 2 reports of the development of a dry powder form of PEG based microparticles for disease-responsive delivery of biologic drugs, intended to be administered by inhalation. The chapter explains the background, significance, motivation, design, as well as the results and discussion of the project. Chapter 3 reports

on the use of PEG based hydrogels to encapsulate murine stem cells for *in vitro* T cell differentiation. The chapter explains the background and motivation for an on-demand *in vitro* T cell source and describes the design and characterization of the hydrogels and the differentiation data obtained. Chapter 4 provides a brief conclusion to this report and its findings and future work needed.

1.4 REFERENCES

[1] L. Brannon-Peppas, "Preparation and Characterization of Crosslinked Hydrophilic Networks," in *Studies in Polymer Science*, vol. Volume 8, Lisa Brannon-Peppas and Ronald S. Harland, Ed. Elsevier, 1990, pp. 45–66.

[2] N. A. Peppas, B. V. Slaughter, and M. A. Kanzelberger, "9.20 - Hydrogels," in *Polymer Science: A Comprehensive Reference*, Editors-in-Chief: Krzysztof Matyjaszewski and Martin Möller, Eds. Amsterdam: Elsevier, 2012, pp. 385–395.

[3] N. A. Peppas, P. Bures, W. Leobandung, and H. Ichikawa, "Hydrogels in pharmaceutical formulations," *Eur. J. Pharm. Biopharm.*, vol. 50, no. 1, pp. 27–46, Jul. 2000.

[4] K. Y. Lee and D. J. Mooney, "Hydrogels for Tissue Engineering," *Chem. Rev.*, vol. 101, no. 7, pp. 1869–1880, May 2001.

[5] N. A. Peppas, K. B. Keys, M. Torres-Lugo, and A. M. Lowman, "Poly(ethylene glycol)-containing hydrogels in drug delivery," *J. Controlled Release*, vol. 62, no. 1–2, pp. 81–87, Nov. 1999.

[6] M. Ehrbar, S. C. Rizzi, R. G. Schoenmakers, B. San Miguel, J. A. Hubbell, F. E. Weber, and M. P. Lutolf, "Biomolecular Hydrogels Formed and Degraded via Site-

Specific Enzymatic Reactions," *Biomacromolecules*, vol. 8, no. 10, pp. 3000–3007, Sep. 2007.

[7] M. P. Lutolf and J. A. Hubbell, "Synthesis and Physicochemical Characterization of End-Linked Poly(ethylene glycol)-co-peptide Hydrogels Formed by Michael-Type Addition," *Biomacromolecules*, vol. 4, no. 3, pp. 713–722, Feb. 2003.

[8] J. Zhang, A. Skardal, and G. D. Prestwich, "Engineered extracellular matrices with cleavable crosslinkers for cell expansion and easy cell recovery," *Biomaterials*, vol. 29, no. 34, pp. 4521–4531, Dec. 2008.

[9] X. Zheng Shu, Y. Liu, F. S. Palumbo, Y. Luo, and G. D. Prestwich, "In situ crosslinkable hyaluronan hydrogels for tissue engineering," *Biomaterials*, vol. 25, no. 7–8, pp. 1339–1348, Mar. 2004.

Chapter 2: Formulation of Disease-Responsive Hydrogel Microparticles for Inhalation

2.1 Background and Significance

The applications of hydrogels in the biomedical field have greatly increased over recent years. One area of research that has shown great interest for hydrogel technology is drug delivery for therapeutic agents. With the increase in need for drug and protein delivery formulations, hydrogels offer targeted, site-specific, controlled release [1]–[3]. Specifically, PEG is one of the most extensively used polymers in hydrogel studies due to its high water-solubility, low toxicity, high biocompatibility and stealth properties [4]. This report focuses on a swellable microcarrier system of degradable microgels designed to encapsulate therapeutic agents for pulmonary administration. The microgels are synthesized by crosslinking PEG with a peptide sequence during a water-in-oil emulsion process, adapted from Wanakule et al. [5]. Further, the microgels undergo freeze-drying in the presence of excipients and are formulated for dry powder inhalation. The microgels are designed to release encapsulated drug via enzymatic degradation of the peptide sequence, which can be tailored to specific disease enzymes. In this report a trypsin sensitive peptide sequence is used as a model peptide.

2.1.1 Motivation

The field of pulmonary delivery of therapeutic agents is greatly expanding for both systemic and local delivery to address the needs of a variety of diseases including asthma, pulmonary fibrosis, airway allergy, growth deficiency, and diabetes [6]. Pulmonary inhalation is a noninvasive means of delivery that offers several advantages over other alternative delivery routes. For systemic delivery, these advantages include bypassing the first-pass effect, large alveolar surface area and low thickness epithelial barrier for drug adsorption, and extensive vascularization [4]. Pulmonary delivery offers

a more effective means of delivery for many drugs that are poorly absorbed from the gastrointestinal tract or are presystemically metabolized [7]. For local targeting of the lungs, such as for Chronic Respiratory Diseases (CRDs), delivery through the lung achieves efficient delivery at the site of action with lower doses while avoiding systemic adverse drug reactions and cytotoxic effects [7]. Ultimately, by improving delivery, lowering dosage, and minimizing adverse reactions, the system has the potential to provide an effective and economical means of delivery that improves patient quality of life and compliance.

However, there are many challenges to designing a pulmonary delivery system that is capable of delivering therapeutics in an efficient and effective manner. For instance, many traditional drugs for inhalation have low respirable fractions due to particle size or aggregation. Also, due to efficient local clearance mechanisms, the resident time of particles in the lung is brief [7], [8].

This project attempts to develop a dry powder formulation of microgel carriers with key characteristics for pulmonary drug delivery, namely efficient aerodynamic delivery to airway epithelial cells through small particle size (i), increased deposition and avoidance of macrophage clearance due to enhanced swelling particle size (ii), and enzyme triggered degradation of microgels for site-specific release of drug (iii).

2.1.2 Drug Delivery of Biologic Drugs

Biologic drugs are increasingly being used in pharmaceutical formulations for a wide array of diseases and conditions. Inhalation is a non-invasive, needle-free approach for the administration of systemic acting proteins and peptides. The PEG and peptide components are crosslinked via conjugate addition reaction that allows the microgels to be synthesized in mild conditions without any UV, high temperatures, or organic

solvents thereby allowing the encapsulation of biologic drugs without risk of potential denaturation [5], [9]. The Hubbell group have successfully used Michael-type addition reactions to form PEG based hydrogels [10]. Our microgels are then prepared for a dry powder inhaler. Dry powders are attractive because they offer the long term physio-chemical stability of the drugs that is not as easily attained in solution [11].

2.1.3 Disease-Responsive Drug Delivery

The aim of controlled release systems is to control the delivery of drugs at target sites and at effective concentrations for a specified duration of time. It is the goal to deliver bioactive molecules within a therapeutic range, below the toxic threshold and above the minimum effective concentration. There are many methods in literature and practice to drive the release of drugs in a controlled manner, such as diffusion, bioerosion, and stimuli-responsive systems [12]. For this system, we chose to create microgels that are stimuli-responsive. Stimuli-responsive systems deliver drugs only when and where they are needed [13]–[15]. This spatial and temporal response is often controlled by physiochemical changes in the carrier's microenvironment. Examples of triggers to cause drug release are pH, temperature, light, or enzymes [16]. By using disease-specific release, the drug can be released in response to specific pathological cues thus making them tailored for a disease. One hydrogel design is to incorporate an enzyme-cleavable peptide sequence into the network structure which will thereby cleave and release the encapsulated drug in response to enzyme exposure. Ehrbar et al. used polymeric hydrogel biomaterials that were degraded via site-specific enzymatic reactions [16]. Our microgel system is designed to release encapsulated drug through enzymatic cleavage of peptide sequences within the microgel network.

In order for the microgel system to function with disease-responsive release, it must remain present in the lungs for a considerable duration of time until the disease specific enzyme initiates the drug release. However, efficiency of local clearance mechanisms by alveolar macrophages is a major challenge in pulmonary drug delivery. To increase the length of time microcarriers are present in the lung, the microgel system offers swelling capabilities to reduce likelihood of undergoing macrophage phagocytosis. To avoid uptake, particles should be greater than 6 μm in geometric diameter [4], [17]. However, to be respirable, the target range is 0.5 to 5 μm in aerodynamic diameter [4]. The microgel system allows us to design dry inhalable particles within the respirable range of aerodynamic diameter but then swell upon deposition within the lung to avoid local clearance. The microgels then degrade upon exposure to disease-specific enzymes, delivering biologic drugs when and where they need to be.

2.1.4 Formulation for DPI Systems

Dry powder inhalers (DPIs) are greatly researched due to their ability to deliver high doses. They offer great advantages over alternative devices for pulmonary delivery such as nebulizers and metered dose inhalers (MDIs). DPIs use powder technology to disperse solid formulations as an aerosol in a patient's inspiratory airflow. There is no need for coordinating between actuation and inhalation and they require no propellant [18].

Dry powders offer greater stability compared to liquid formulations. By removing water from formulations, physical and chemical stability is more easily achieved. Freeze-drying, or lyophilization, is one of the most common methods to convert suspensions into solids [19]. The process involves at minimum two steps. The initial is the freezing step where the liquid suspension is cooled and the solution or suspension is made a solid one.

The second step is the drying step. The drying process involves sublimination of the ice from the frozen suspension and any water from the system. Here, the use of liquid nitrogen is used to snap freeze the microgels made during emulsion and left in suspension of water and any excipient sugar. The drying steps take place over at least 48 hours on a lyophilizer that keeps the entire product under vacuum during drying.

The use of the excipient sugars is extremely important in the formulation. The freeze-drying process itself, while producing a more stable product, may induce many stresses on the microgels and the drugs they carry. The formation of ice crystals may create mechanical stresses on the system. In addition, the drying process often causes the particles to clump and aggregate making it difficult to produce a free flowing powder capable of reaching the deep lungs. Therefore, excipients to protect the product from freeze-drying stresses (cryoprotectants) were added. Common excipients used as stabilizers and cyroprotectants are sugars and include sucrose, lactose, glucose, and mannitol as well as trehalose, glycerol, and sorbitol. These excipients have all been utilized as excipients in freeze-drying of pharmaceutical products to protect the product during the freezing and the drying stresses [19]–[21]. Of these, lactose and mannitol have demonstrated as effective cryoprotectants for polymer based microparticles and were utilized in this report. Lactose has been approved and is the most commonly used in accepted DPI formulations while mannitol is also approved for formulations such as Exubera® [18]. In general, the microparticles are immobilized within a matrix of cryoprotectant that acts as a shield to the mechanical stresses of the ice crystal formation during the lyophilization process. Also this matrix helps protect the particles from aggregation. It has been proposed that individual particles are isolated by the cryoprotectant in the unfrozen fraction and that this spatial separation of particles is sufficient to prevent aggregation [19]. Saez et al. reported after attempting various

cryoprotectant agents that sucrose and glucose at a concentration of 20% was acceptable in stabilizing effects with no aggregation on poly (D,L-lactic-glycolic) (PLGA) and polycaprolactone (PCL) nanoparticles respectively [22]. The concentration of the sugar to the microgel affects both the stabilization and ability to produce a free flowing powder [19], [23].

Disaggregation is a key design aspect to free-flowing microparticles capable of reaching the lung. Particles targeted for the deep lung must have aerodynamic diameters in the rage of 0.5-5 μm to successfully pass through the mouth, throat, and conducting airways. Additionally, they must not be below 0.5 μm or they risk being exhaled before reaching the deep lung [4], [7], [18]. Aggregation during the freeze-drying process presents the greatest risk of inhibiting the microgels from achieving this target aerodynamic diameter range.

2.2 MATERIALS AND METHODS

2.2.1 Hydrogel Synthesis and Preparation

2.2.1.1 Bulk hydrogel and microgel synthesis

Microgels were synthesized using an adapted method of Michael addition cross-linking during (water-in-oil) emulsion (MADE) [5]. The microgels were synthesized from four arm poly(ethylene glycol) acrylate (PEG-4-acr, Laysan Bio, Arab, AL) of 10,000 kDa and di-sulfhydryl peptide sequence CGRGGC (CHI Scientific, Maynard, MA), acting as the enzyme sensitive microgel component for degradation. Equimolar amounts (sulfhydryl:acrylate) of the peptide and PEG-4-acr were dissolved separately into 0.3 M triethanolamine (Sigma-Aldrich, St. Louis, MO) buffer at pH 7.8. The peptide was dissolved into 15μL of buffer and the PEG-4-acr was dissolved into 85 μL for a total combined concentration of 60% (w/v). The two solutions were combined, quickly

mixed, and transferred to 15 mL of paraffin oil with 1% (v/v) Span80/Tween80 surfactant combination of HLB=5. The emulsion process then occurred using a Polytron PT 3100 homogenizer at 3000 rpm for 3 min, while the entire mixture was immersed in a hot water bath at 40-50 °C. The emulsion was then incubated at 37 °C overnight to allow for sufficient time for the crosslinking to complete and the microgels to form within the emulsions.

To prepare bulk hydrogels, rather than micro-sized hydrogels (microgels) from emulsion, the peptide and PEG-4-acr components were combined at 60% (w/v) in 0.3 M triethanolamine buffer directly into silicon molds. The hydrogels were incubated overnight at 37 °C.

2.2.1.2 Washing and drying steps

After the incubation step to allow for completion of crosslinking overnight, the mixture was centrifuged at 10,000xg for 20min, the supernatant discarded, and re-suspended in 20-25 mL of paraffin oil and vortexted. The new mixture was then left rotating at room temperature for at least 2 hours. After this initial oil wash, three water washes were performed to remove any residual surfactant, oil, and un-reacted material. The washes consisted of centrifugation at 21,000 xg for 20 min, removal of supernatant, resuspension of microgels in deoionized water, and vortexing. Following 3 water washes, the microgels were re-suspended in either deionized water, phosphate buffered saline, 100 mM ammonium bicarbonate, or deionized water with excipient mixture for lyophilization (depended on the buffer required for various assays or freeze-drying).

Microgel particles were dried in deionized water or deionized water with excipient sugar of alpha-lactose monohydrate (Sigma-Aldrich, St. Louis, MO), inhalation grade lactose InhaLac® 120 (Meggle Excipients & Technology, Wasserburg, Germany),

or D-mannitol (Sigma-Aldrich, St. Louis, MO) at varying ratios. The final suspension of powders at 6% was mixed thoroughly by pipetting and gentle vortexing for 5 minutes before snap freezing in liquid nitrogen. The samples were placed on the lyophilizer for at least 48 hours to remove all water. After lyophilization, some formulations were transferred to scintillation vials and placed in T2 Turbula blender (GlenMills Inc, Maywood, NJ) or 30 minutes to create a more uniform free-flowing powder.

2.2.1.3 Encapsulation of nanoparticles

To encapsulate nanoparticles into the microgels, creating a nano-in-micro system, nanoparticles were mixed into the PEG-4-acr in 0.3M triethanolamine buffer solution prior to emulsion steps. The PEG-4-acr and the peptide solutions were then combined and the emulsion process, washing, and drying steps were remained exactly the same as described previously. During the course of experiments, nanoparticles used included 20nm Crimson and 40nm Dark Red FluoSpheres (Invitrogen, Carlsbad, CA).

2.2.1.4 Conjugation of fluorescent probe to microgels

Another method of quantifying the fluorescence of microgels was to conjugate the microgels with a fluorescent probe rather than encapsulating nanoparticles. This method was used for NGI data and *in vivo* experiments. The conjugation step occurred after the oil wash and water washes but before lyophilization of microgels. For *in vivo* experiments and homogenization data Alexa Fluor ® 633 Carboxylic Acid Succcimidyl Ester (AF633-SE, Life Technologies, Carlsbad, CA) were conjugated onto the primary amines via its carboxylic acid group. AF633-SE was added to the microgels as per manufacturer's instructions and left rotating at room temperature for 2 hours. Following conjugation, additional water washes were performed to remove all unreacted materials and the solution was dialyzed with at least three dialysis changes in one liter of de-

ionized water for at least 12 hours total. For NGI experiments, the microgels were conjugated with 5(6)-Carboxyfluorescein succinimidyl ester (FAM-SE, Invitrogen, Carlsbad, CA) mixed isomers. Once again, the mixture was rotated at room temperature for 2 hours to allow completion of conjugation followed by at three additional water washes.

2.2.2 *In vitro* Characterization of Lyophilized Hydrogels

2.2.2.1 Size and morphology

Microgels were sized using a Malvern Zen1600 Zetasizer (Malver Instruments Ltd., Worcestershire, United Kingdom). 2 mg of microgels were dispersed in paraffin oil or water to get particle size and distribution from the accompanying instrument software. Microgels were also observed via SEM (Institute for Cellular and Molecular Biology Core Facility, University of Texas at Austin). The lyophilized microgels, with or without excipient, were coated with 12nm Pt/Pd for SEM imaging. Images were analyzed on the GNU Image Manipulation Program (GIMP) software.

2.2.2.2 Raman spectroscopy

Raman spectroscopy (University of Texas at Austin, Austin, TX) was used to investigate the vibrational modes in the polymers which occur in the frequency spectrum between 600-4000 cm^{-1}. Raman spectroscopy irradiates in the UV/Vis region, in which water does not absorb, and is therefore suitable for hydrogel systems that contain water. Tested samples included, acrylated PEG, peptide, relaxed hydrogels, hydrogels swollen in PBS, lyophilized hydrogels, and lyophilized hydrogels swollen in PBS. The Raman spectrometer was set up at 50x magnification and laser power adjusted between 50% and 10% for each sample.

2.2.2.3 Swelling properties

Swelling studies were performed on hydrogels by weighing after gelation and crosslinking. The hydrogels were allowed to swell at 37°C in PBS (pH 7.4) on a slow speed rocker. At regular time intervals, hydrogels were removed from solution. Excess water droplets on hydrogels were removed by gentle blotting of gel on KimWipe. The weight of the swollen gels were recorded and swelling ratio was determined.

2.2.2.4 Enzyme-triggered degradation and nanoparticle release

Hydrogel degradation profiles of bulk gels were performed in similar fashion to the swelling study but the hydrogels were placed in solutions containing various concentration of trypsin (Sigma-Alrdrich, St. Louis, MO). Weight measurements were taken at respective time points of the hydrogels upon exposure to enzyme. Various trypsin concentrations (8.125 U/mL, 16.25 U/mL, and 32.5 U/mL) were used. Release studies were performed by first encapsulating nanoparticles within the microgel system (as previously described). The microgels were exposed to 10 U/mL trypsin and at regular time intervals, the microgel suspension was centrifuged, the supernatant removed, and fluorescence readings were taken to assess the release of nanoparticles.

2.2.3 *In vitro* Aerosolization and Pulmonary Deposition

A Next Generation Impactor, NGI, (MSP Corporation, Shoreview, MN) was used at the University of Texas at Austin TherapeUTex facilities (Austin, TX) for *in vitro* aerosolization studies. In each procedure, a size 3 HPMC capsule (Vcaps®, Capsugel, Morristown, NJ) was loaded with approximately 10mg of powder. The capsule was punctured in a handheld inhaler (Spiriva® HandiHaler®, Boehringer Ingelheim Pharmaceuticals, Ingelheim am Rhein, Germany) and placed on an adapter to the NGI before inhalation was stimulated. The airflow rate was set to 60 L/min for duration of 4

seconds, thereby resulting in a 4 L inspiration volume. Each run consisted of 3 capsules, each filled with 3 different batches (n=3) of microgels in sequence. The plates of the NGI were coated with 5% Tween 80 in methanol and then rinsed after powder deposition with water. The microgels for aerosolization studies were conjugated with 5(6)-Carboxyfluorescein, succinimidyl ester (FAM-SE, Invitrogen, Carlsbad, CA) mixed isomers. The powders were extracted from the various stages of the NGI through rigorous rinsing with water. The extracted solution from the NGI was then measured for deposited microgels by fluorescence at (wavelength) using a BioTek plate reader. Additional analysis was performed using the Copley Inhaler Testing Data Analysis Software (Copley Scientific, Nottingham, United Kingdom) accompanying NGI.

2.2.4 *In vivo* Pulmonary Deposition (murine lung homogenization)

In vivo studies were repeated for this report with slight modifications to method of homogenization. Microgels conjugated with AF-633 were directly introduced into 8-10 week old BALB/c female mouse (Jackson Laboratories, Bar Harbor, ME) lungs using a Penn-Century MicroSprayer device, commonly used to deliver test formulations to rodents in vivo [24], [25]. Each mouse was delivered a dose of 0.1mg of particles in 50 μL of PBS. The doses were delivered by Prinda Wanakule at the University of Texas at Austin Animal Resource Center (Austin, Texas). At specified time points, mice were sacrificed the lungs extracted for homogenization. The trachea and esophagus were removed before mincing the lungs with scissors and put into a centrifuge tube with 3 mL of tissue lysis buffer (TLB) composed of 50 mM Tris-HCl, 150 mM NaCl, and 0.1% Triton X-100. The lungs in TLB were then homogenized for 1 minute or until all lung chunks were homogenized. After homogenization, 4 mg/mL of trypsin was added and the lungs were left on a rocker at 37°C for 72 hours. The fluorescence was then read on a

plate reader (BioTek) to determine microgel concentration in the lungs. The samples were compared to standard curve prepared with mouse lungs and known concentrations of AF-633 conjugated microgels.

2.3 Results and Discussion

2.3.1 Hydrogel Synthesis and Characterization

The synthesis protocol for formation of microgels using MADE technique was varied initially. Variable parameters included homogenization speed, time, washing steps, and drying steps. For example, ethanol washes were attempted in place of water washes to rinse particles of any residual oil and surfactant. However it was determined that water produced the cleaner, more free-flowing powder after lyophilization. Also, the additional overnight oil wash was added as it produced microgels with less residual surfactant. Various drying procedures were tested including drying samples under low pressure with a bench top Nalgene vacuum chamber. This method produced microgels with more smooth and spherical morphology, but the samples were still sticky, aggregated, and not free-flowing. The protocol stated above was determined to be the optimal synthesis procedure.

Lyophilized microgel morphologies and sizes with and without excipients were observed under SEM, as shown in **Figure 2.1**. Plain microgels with no excipient show mostly spherical shape with a wrinkled surface (**Figure 2.1A-C**). The rough exterior is most likely a result of the high vacuum during lyophilization causing the microgel to slightly collapse on itself. Previous studies have shown a porous microstructure within the microgels which supports this theory of some collapse during lyophilization [5]. In **Figure 2.1C** it is also apparent that there is some degree of fusion between the microgels after lyophilization. The addition of lactose to the drying steps, as described before,

created matrix-like, web structures around the microgels. By immobilizing the microgels in a matrix of cryoprotectant, the sugar acts as protection to the microgels from the mechanical stresses induced during the lyophilization process as well as preventing aggregation. Theoretically, this matrix of microgels and sugar will disperse upon actuation in a DPI device releasing individualized microparticles. The SEM images of microgels lyophilized in lactose solution (**Figure 2.1 D,E**) shows the matrix-like structure as well as many particles that have retained a smooth spherical shape.

The SEM images also appear to confirm the sizes determined using a Malvern Zen1600 Zetasizer, shown in **Table 2.1**. Lyophilized microgels were sized while dispersed in paraffin oil showing a relaxed state with average geometric diameter of 2.983±2.309 μm. Lophilized microgels were also dispersed in water for approximately 20 minutes before sizing. The average geometric diameter increased to 3.529±2.878 μm. This increase is likely due to the swelling of the microgels within water. The diameters of the lyophilized microgels are higher than those measured of microgels that had not undergone freeze drying. This indicates that the microgels may be aggregating or fusing during the freeze drying process.

Table 2.1 Geometric diameter (mean±standard deviation) of microgels in different suspension mediums

	Lyophilized microgels	Control microgels
Suspended in Paraffin oil (relaxed state)	2.983±2.309 μm	1.660±1.362 μm
Suspended in D.I. water (swollen state)	3.529±2.878 μm	1.893±2.729 μm

In order to further diagnose any variations between relaxed hydrogels and the freeze-dried hydrogels, Raman spectroscopy studies were performed (**Figure 2.2**). Raman spectroscopy provides information on molecular vibrations to determine the

molecular composition of the hydrogels. The samples tested included PEG-4-acr; CGKCGGC peptide; non-swollen, relaxed hydrogel; swollen hydrogel; non-swollen, lyophilized hydrogel; swollen, lyophilized hydrogel. The swollen hydrogels were allowed to swell in PBS for 1 hour at 37 °C with continuous rocking. The results shown depicts all the samples tested, displaying varying intensities but consistent peaks among the samples within each condition. The lyophilized hydrogel, without any swelling, resulted in too dense of matter for the light to penetrate, and no peaks were able to be determined (data not shown). Peaks of interest were seen at 1640 in the PEG-4-acr sample representing the double bond between carbons (C=C) and also seen at 1640 in the swollen control hydrogels. However, this peak is not present in the swollen lyophilized hydrogels. This difference between the control and lyophilized gels shows the change that occurs during the freeze drying process on a molecular level. To assure that the hydrogels still perform similarly in swelling, degrading, release rate, and morphology, assays were performed on the lyophilized hydrogels, as detailed in the proceeding sections. Also, the Raman data reveals the sulfhydryl group (S-H) is represented in the peak at 2570 in the peptide sequence but is not seen in any of the gel. This is possibly because of the small quantity remaining after the crosslinking occurs.

Characterization of the lyophilized microgels was performed to compare their behavior to normal, relaxed microgels (not in dry state). Since Raman spectroscopy data points to the possibility of small differences in molecular composition, studies were performed to understand whether the lyophilized hydrogels were still able to perform the necessary functions for a pulmonary microcarrier system. Namely, we first studied the swelling and degradation properties of the hydrogels, which are central to their designed function as pulmonary triggered-release gels.

For ease of measurements, these initial experiments to compare the behavior of freeze-dried hydrogels with the previously verified behavior of the relaxed, non-lyophilized hydrogels were performed with bulk gels rather than the microgels. The average swelling ratio (q) was defined as a ratio of the weight of swollen gels to the initial weight after gelation. The hydrogels were allowed to swell at 37 °C in PBS on a slow speed rocker and weighed at regular time intervals.

Swelling Ratio, $q = Weight_{swollen} / Weight_{initial}$

The results, in **Figure 2.3**, show the dried hydrogels experienced delayed swelling compared to the relaxed, control hydrogels. The swelling of the lyophilized hydrogels were consistent and remained in a swollen state for an extended period of time, up to nearly two weeks. The gravimetric measurements used to determine the swelling ratio may have contributed to the decline in the mass for both groups of gels, since the hydrogels were dabbed with a KimWipe to remove excess water before taking the weight measurements, small amount of hydrogel residuals may have been lost each time. Even still, the lyophilized hydrogels performed well in the sense that they showed they are capable of swelling to the same degree and longer extent then relaxed hydrogels.

A key design element of the hydrogels is their enzymatically triggered release. The hydrogels were synthesized by Michael addition of PEG-4-acr and an enzyme sensitive peptide. The specific peptide sequence chosen for in vitro studies is sensitive to trypsin. Previously, optical trapping techniques were used to capture, view, and track microgels rapidly degrading in the presence of enzyme [5]. The time-lapse images showed the various stages of enzyme-mediated degradation.

To confirm enzyme-mediated degradation of bulk hydrogels that had undergone freeze-drying, weight measurements were taken at respective time points of the hydrogels upon exposure to enzyme. We continued to use trypsin as the model enzyme able to

cleave the peptide sequence cross-linked in the hydrogels. The degradation of the bulk hydrogels upon exposure to trypsin was measured by a weight ratio. **Figure 2.4** shows the degradation profiles of lyophilized hydrogels (**Figure 2.4B**) and control, relaxed hydrogels (**Figure 2.4A**). Various trypsin concentrations (8.125 U/mL, 16.25 U/mL, and 32.5 U/mL) were used to assess the dependence of trypsin concentration on degree of degradation over the course of only 5 hours.

The data revealed that although lyophilized bulk hydrogels showed a tendency to degrade at a slightly slower rate than relaxed hydrogels, the degradation profiles were not significantly different. The data also confirmed that the degradation rate was dependent on the trypsin concentration, with higher trypsin activity leading to increased degradation. The degradation was very apparent in trypsin concentration of 16.25 U/mL and 32.5 U/mL, although the trypsin concentration of 8.125 U/mL did not result in degradation at least in the 5 hours of measurements.

The degradation of the microgels was assessed also by weight ratios. Trypsin was added to the microgels at a concentration of 16.25 USP U/mL, a level well below normal physiological ranges [26]. The measurements were taken out over 7 days in order to fully measure full degradation of microgels. **Figure 2.5** shows the degradation as a weight ratio of relaxed (non-lyophilized) and lyophilized microgels. The protocol adopted involved weighing the particles in centrifugal filters, filtering out degraded particles and weighing the particles that remained in the filter at each time point. The weight ratio profiles remained similar between the dried and wet microgels and after 96 hours (4 days) the lyophilized microgels reached near full degradation while the relaxed microgels reached that state only after 168 hours (7 days).

Enzyme-mediated release studies were performed to follow up on the degradation weight measurements. In order to fluorescently trace the release of encapsulated nanoparticles, 20nm and 40nm fluorescently marked polystyrene nanoparticles were used. The microgels with the nanoparticles encapsulated were continuously rocked in ammonium biocarbonate buffer with either 10USP U/mL trypsin in HCl or no trypsin, as a control group. At pre-determined time points, the microgels were centrifuged and the supernatant was measured for fluorescence indicating released nanoparticles.

All microgels in this study were lyophilized after encapsulation. Trypsin was added to the microgels at a concentration of 10 USP U/mL. **Figure 2.6A** depicts the cumulative release of the 40nm nanoparticles (Dark Red FluoSpheres®) from the microgels over 12 hours. The results show an increased release from lyophilized microgels exposed to 10 USP U/mL of trypsin than those exposed to no trypsin. After 12 hours, the microgels with trypsin released an average of 86.98 ± 3.59 % of total encapsulated nanoparticles. The control group of lyophilized microgels was not exposed to trypsin and released 40.32 ± 13.92% of nanoparticles after 12 hours. Although this release can be passive release without enzyme-triggered degradation, it is also partially attributed to the study's protocol of centrifuging the microgels causing stress and potential release of encapsulated nanoparticles. However, a minor extent of non-specific degradation cannot be ruled out. The study was repeated with 20nm nanoparticles (Crimson FluoSpheres®) (**Figure 2.6B)**. After 12 hours, the microgels released 38.90 ± 12.08 % of total encapsulated 20nm nanoparticles. The control group released only 17.09 ± 1.26% of total encapsulated 20nm nanoparticles.

2.3.2 Formulation for DPI System

Freeze-drying process was used to prepare inhalable powder forms of the microgels. This method has been considered suitable for long-term stability of particles [19]. However, the freeze-drying process can result in aggregation, fusion, and mechanical stresses of ice crystals causing destabilization of the microgels [7]. Sugars are generally used as cryoprotectants and stabilizers to protect the particles from the freezing and drying stresses. Coarse lactose and mannitol were initially chosen to act as stabilizers and as bulking agents for the resulting powder. Aqueous solutions containing the microgels and excipient sugars were prepared in water with a total powder mass of 6% (w/v) then freeze-dried for at least 48 hours. Powder formulations consisted of microgel/mannitol or microgel/lactose in weight ratios of 1:1 and 1:5.

The NGI consists of an initial inhaler/device and adapter set-up followed by induction port and preseparator representing powder deposited in mouth and throat followed by seven plates and the micro-orifice collector (MOC) as the eight plate. The diameters, μm, of the particles deposited at each plate at flow rate of 60 L/min are shown in **Table 2.2**.

Table 2.2 Diameters of particles deposited on NGI plates at flow rate of 60 L/min

NGI Plate:	1	2	3	4	5	6	7	8 (MOC)
Diameter, μm, of deposited particles:	8.06	4.46	2.82	1.66	0.94	0.55	0.34	<0.34

The emitted dose is defined as the percentage of total powder mass discharged from the capsule upon breath activation at 60L/min. It was determined gravimetrically and is expressed as

$$ED\% = \left(\frac{Initial\ mass\ in\ capusle - Final\ mass\ in\ capsule}{Initial\ mass\ in\ capsule}\right) \times 100$$

All the powders successfully showed emitted doses of near 100% indicating breath actuation was able to disaggregate the particles upon inhalation and there was low adherence of particles to the capsule shell.

Further the fine particle fraction (FPF), mass medium aerodynamic diameter (MMAD), and geometric standard deviation (GSD) were calculated using the Copley Inhaler Testing Data Analysis Software (Copley Scientific). The FPF represents the percentage of particles less than or equal to 5 μm, indicating the percent of powder that is able to be inhaled into the lungs.

None of the initial formulations of microgels with mannitol or lactose in 1:1 or 1:5 ratios resulted in the targeted MMADs of less than 5 μm (**Table 2.3**). However the addition of lactose and mannitol did show improved decrease in MMAD than the microgels without any excipient. The microgel/lactose 1:1 formulation proved to have the lowest MMAD of 6.21 μm however both the mannitol formulations showed to have higher FPFs. Still, all the formulations resulted in FPFs of less than 20% showing only a small fraction of the dose of powder will reach the lungs. Better formulation will prevent aggregation of the individual particles during the drying steps as well as particles more easily disaggregated during the inhalation process.

The results of the aerosolization studies with coarse lactose and mannitol indicated a significant need to better tailor the microgels for inhalation. To produce finer powder, inhalation grade lactose (InhaLac® 120, Meggle Excipients & Technology, Wasserburg, Germany) was substituted as the excipient of choice at ratios of microgel to lactose of 1:1, 1:5, 1:10, and 1:20. InhaLac® 120 lactose is sieved lactose designed specifically for use in dry powder inhalers with diameter, d_{50}, of 130 μm, smooth particle surface, narrow particle size distribution, and overall better flowability. Also, an additional step was added to formulation and the powders were blended after dryings and

before loading into the capsules to produce more uniform powders. Powders were removed from lyophilizer then transferred to scintillation vials and placed in T2 Turbula blender for 30 minutes to create a more uniform free-flowing powder.

Data showing the emitted doses of microgel dry powder with inhalation grade lactose (**Figure 2.8A, Figure 2.9A**) show emitted doses at 80% or higher for all formulations indicating that actuation and breath air flow of 60 L/min is sufficient to disaggregate the powder and remove residual powder from device. However, the formulations with inhalation grade lactose and no blending (**Figure 2.8**) displayed poor deposition in the NGI and most of the powder was deposited within the induction port and preseparator components of the NGI, approximately 80% for all the ratios of inhalation lactose. This indicates the microgels were unable to dissociate for the lactose and flow freely deep into the NGI plates. Since such a small amount of the microgels made it into the NGI plates, the MMAD and FPF measurements were unable to be computed accurately but CITDAS software for formulations with 1:1 and 1:10 inhalation grade lactose. However, when the blending step was added in the inhalation grade lactose formulations (**Figure 2.9**) the microgels deposited farther within the NGI and displayed improved aerodynamic properties. All the blended formulations resulted in MMAD of less than 5 μm (**Table 2.3**), although the GSD were very high. Microgel/InhaLac ratio of 1:5 produced the smallest MMAD of 1.812 μm and FPF of 7.041. The microgel/InhaLac 1:10 and 1:20 formulations had slightly higher MMAD, 2.712 μm and 2.453 μm respectively, however, they exhibited higher FPF values, 8.5357% and 12.943% respectively. These two formulations appear to have the greatest range of particle size distribution and the largest fraction of powder proved capable of reaching the deep lung.

Table 2.3 Fine particle fraction (FPF), mass medium aerodynamic diameter (MMAD), and geometric standard deviation (GSD) of microgel formulations

	FPF (%)	MMAD (μm)	GSD
Plain MGs	1.91	7.899	1.419
MG: Mannitol (1:1)	17.017	6.246	6.956
MG: Mannitol (1:5)	6.548	6.956	1.407
MG: Lactose (1:1)	3.711	6.21	1.314
MG: Lactose (1:5)	0.637	7.821	1.48
MG: InhaLac (1:1)	0.562	Unable to accurately measure	
MG: InhaLac (1:5)	1.594	7.612	1.539
MG: InhaLac (1:10)	0.234	Unable to accurately measure	
MG: InhaLac (1:5), blended	7.041	1.812	3.955
MG: InhaLac (1:10), blended	8.357	2.712	6.980
MG: InhaLac (1:20), blended	12.943	2.453	6.603

2.3.3 *In vivo* pulmonary deposition of microgels (lung homogenization)

Although this particular study did not involve lyophilized microgels it still demonstrates the ability of the microgels to be delivered through intratracheal administration to mouse and show low clearance over the course of 2 weeks. This

experiment was performed as a repeat to an earlier experiment with slight modifications. Lung samples were extracted, homogenized, and analyzed for fluorescence levels to indicate retention of AF-633 conjugated microgels. **Figure 2.10** shows the percent of microgels remaining in the lungs in terms, calculated based off of initial dose administered and fluorescence data from a standard curve produced. At day 1, approximately 64% of administered microgels are present in the lungs. The levels of microgel in the lungs decrease over day 1 and 3, down to approximately 38%. At day 7, the presence of microgels is reported to be back up at approximately 66%, however the standard deviations are large and this is still within physiological range. However, the data deviates significantly at day 14 where fluorescence peaks and the calculated percent of microgels remaining in the lungs is greater than 100%. This phenomenon, of the rapid increase of microgel fluorescence, is surprisingly consistent with the initial experiment performed. One possible explanation may be due to human error of dosing the mice whose lungs were homogenized for day 14 or homogenization error. Another explanation, and possibly more likely scenario to explain the earlier experiment as well, is that the AF-633 conjugated microgels experienced fluorescent quenching. The study will have to be repeated in the future with changes to the protocol to avoid any errors. The data is still helpful in showing that the microgels at least maintained some presence in the lungs throughout the duration of 14 days.

Figure 2.1 SEM images of lyophilized microgels

SEM images of microgels after undergoing 48 hours of lyophilization without any excipients (A-C) or with lactose as a cryoprotectant at a 1:1 ratio to microgel (D-E).

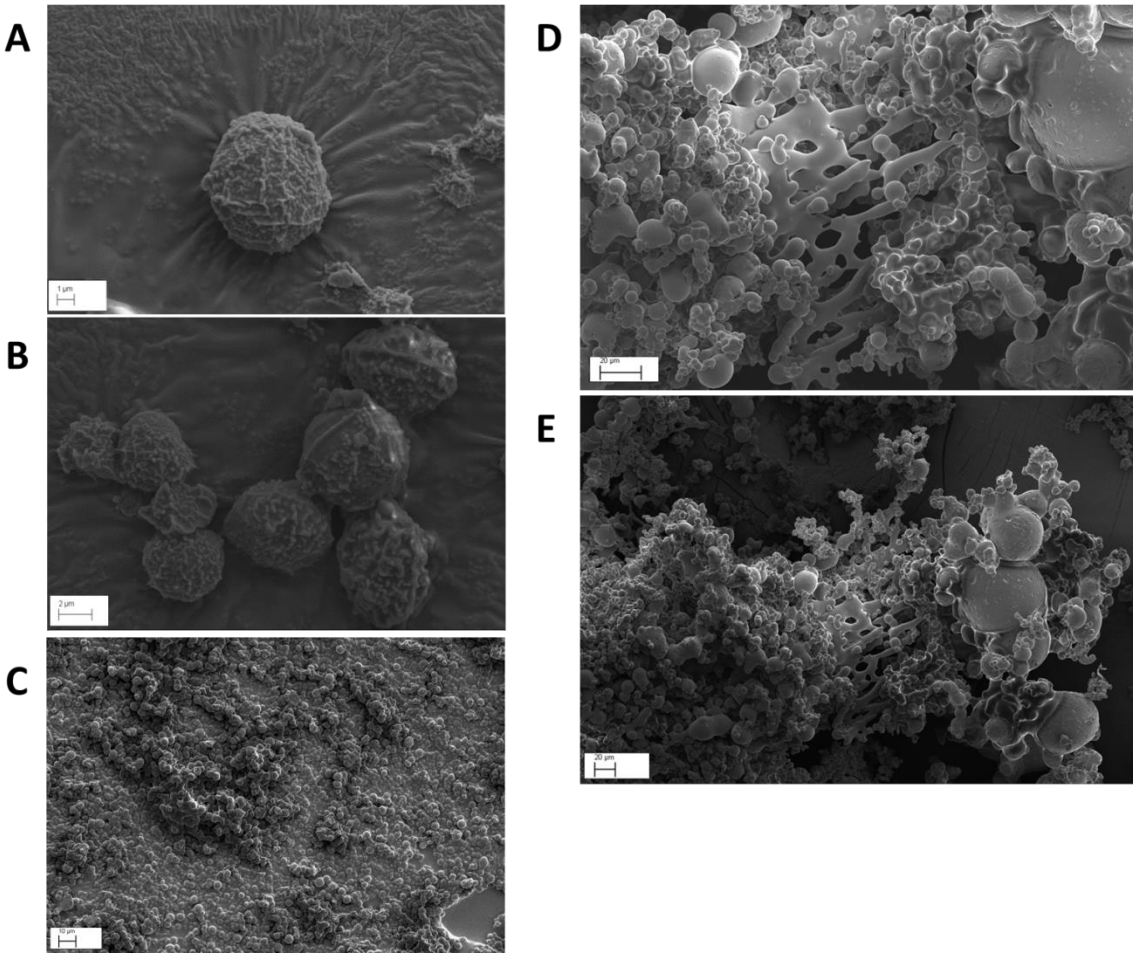

Figure 2.2 Raman spectroscopy data from hydrogels and components

Raman spectroscopy data provides information on molecular vibrations to determine the molecular composition of the hydrogels. The samples tested included PEG-4-acr, CGKCGGC peptide, swollen hydrogel, and swollen, lyophilized hydrogel. The swollen hydrogels were allowed to swell in PBS for 1 hour at 37 °C with continuous rocking. The results shown depicts all the samples tested, displaying varying intensities but consistent peaks among the samples within each condition.

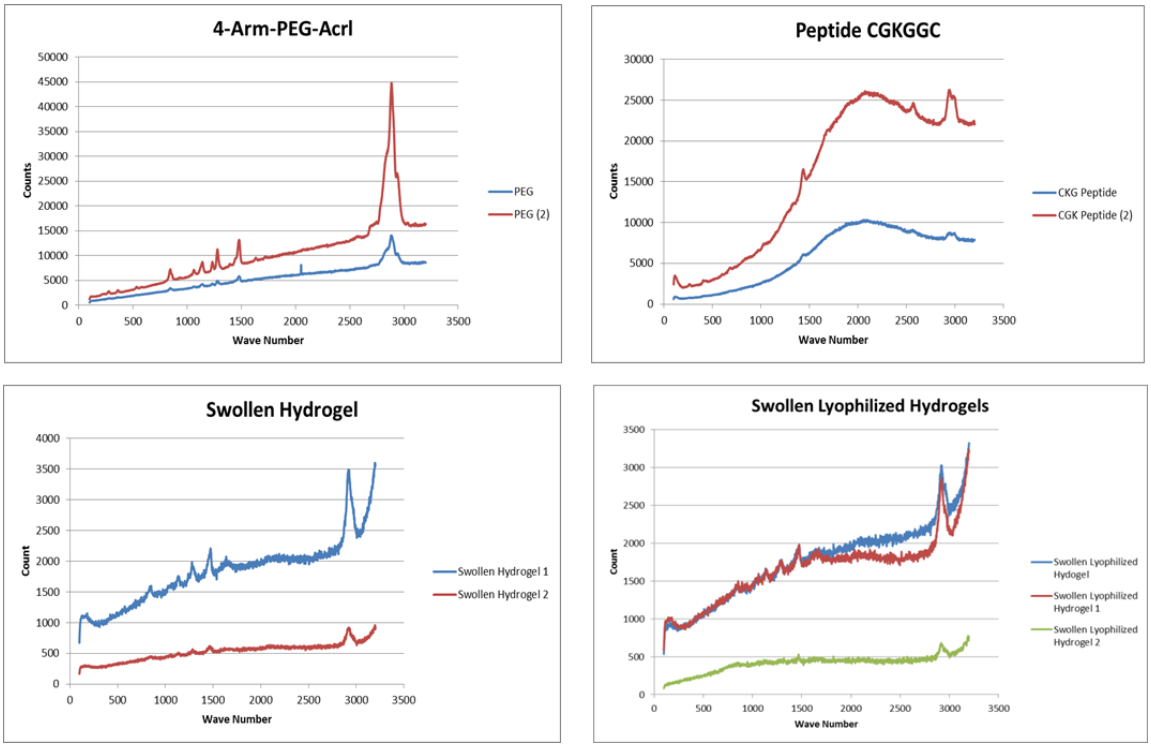

Figure 2.3 Swelling profile of hydrogels

The average swelling ratio (q) was defined as a ratio of the weight of swollen gels to the initial weight after gelation. The hydrogels were allowed to swell at 37 °C in PBS on a slow speed rocker and weighed at regular time intervals.

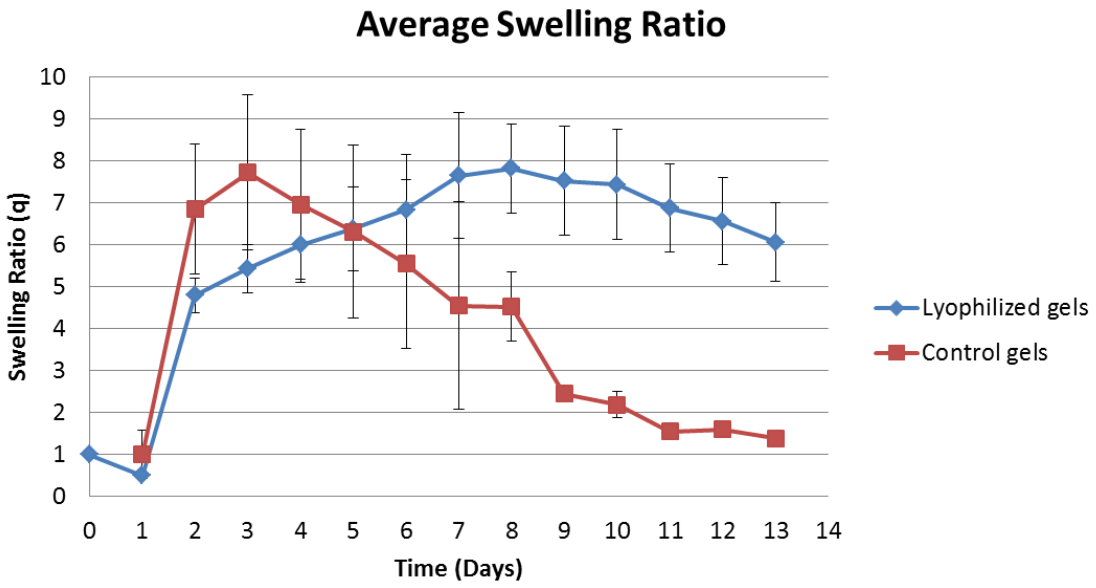

Figure 2.4 Degradation profiles of bulk hydrogels in varying trypsin concentrations

Weight ratios, q, were used to assess degradation of lyophilized hydrogels (B) and control, relaxed hydrogels (A). Various trypsin concentrations (8.125 U/mL, 16.25 U/mL, and 32.5 U/mL) were used to show the dependence of trypsin concentration on degree of degradation over the course of only 5 hours.

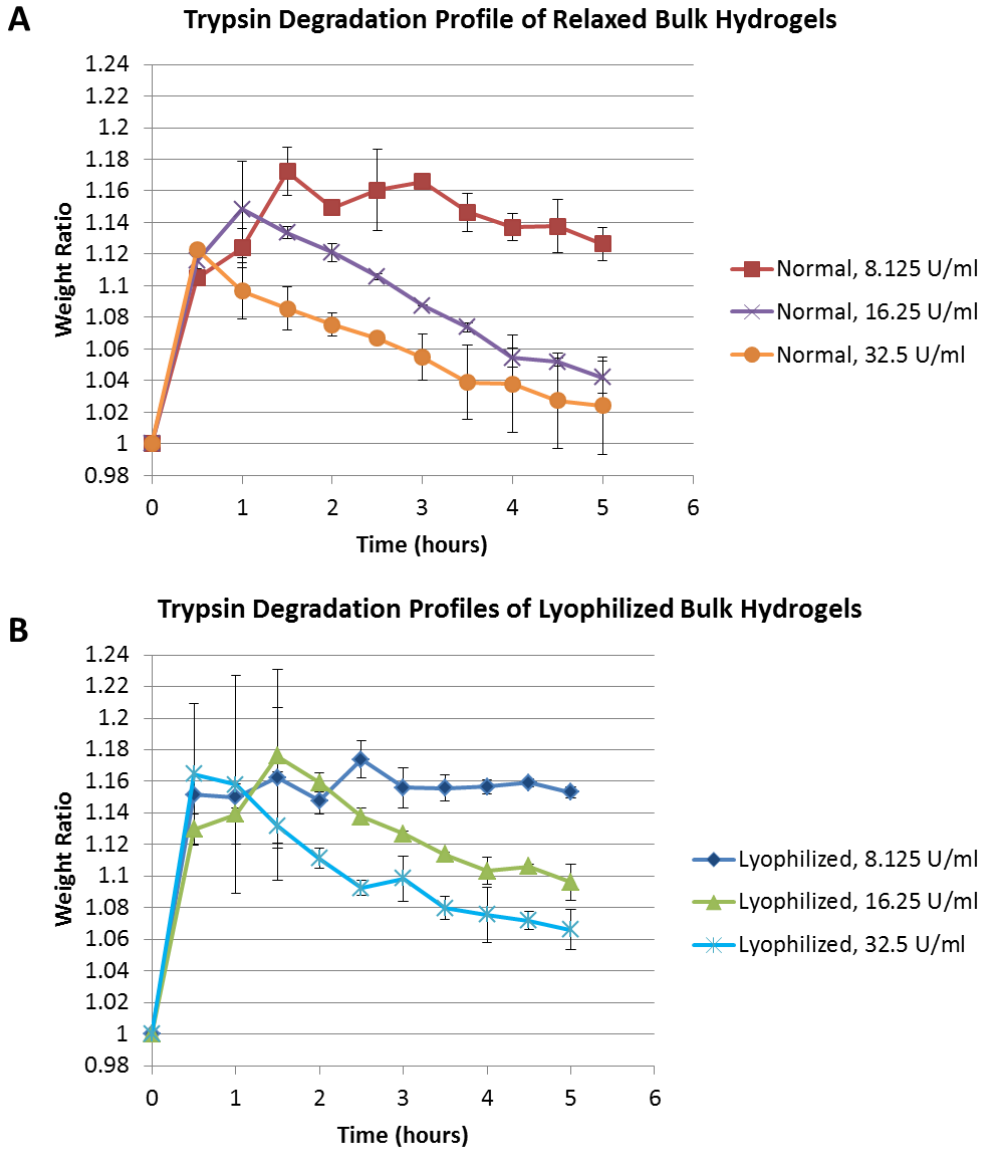

Figure 2.5 Degradation profiles of microgels

Weight ratios, q, were used to assess degradation of lyophilized and relaxed microgels in 16.25 U/mL trypsin over 7 days. The weight ratio dips down to approximately 0, showing complete degradation of the microgels.

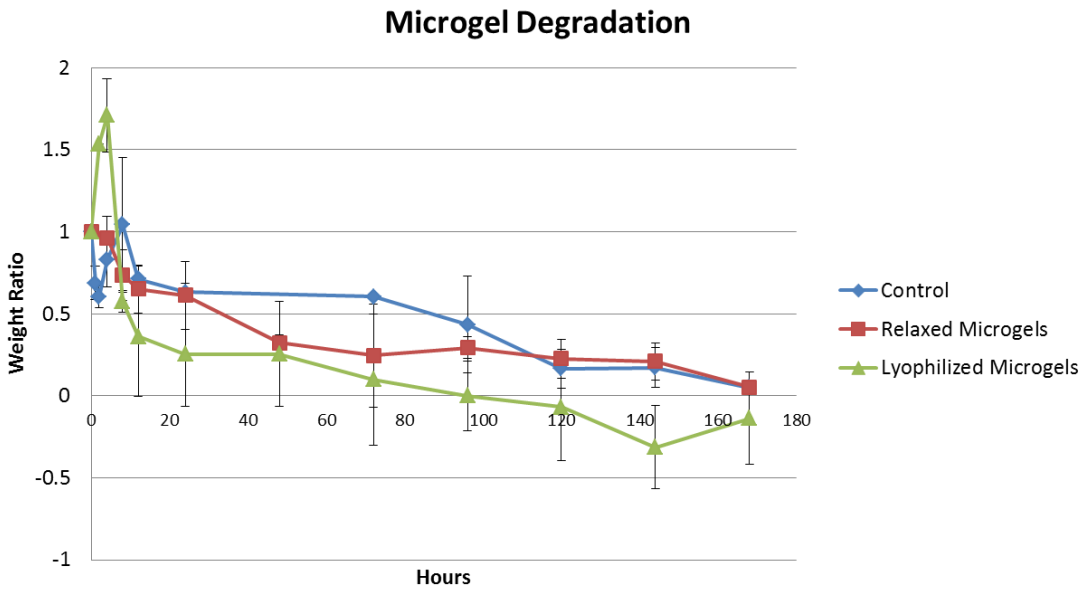

Figure 2.6 Microgel release of encapsulated fluorescent polystyrene nanoparticles

The cumulative release of fluorescent 40nm Dark Red FluoSpheres® (A) and 20nm Crimson FluoSpheres® (B) encapsulated within lyophilized microgels exposed to 10 USP U/mL of trypsin and control microgels exposed to no trypsin.

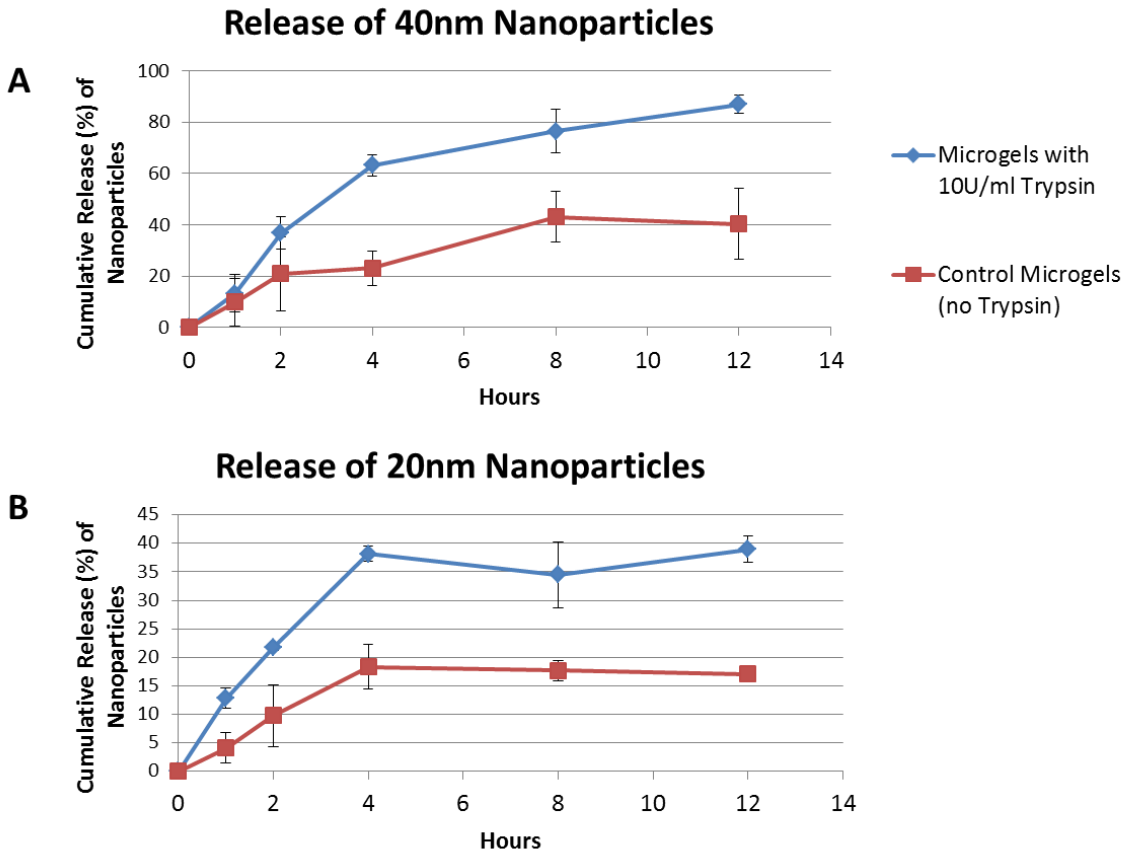

Figure 2.7 Formulation development 1: DPI emitted dose and microgel NGI distribution

The microgels were lyophilized with mannitol or lactose then loaded into HPMC size 3 capsules, actuated within the DPI device, and deposited within the NGI at a flow rate of 60 L/min for 4 seconds. Each NGI run consisted of three microgel-loaded capsule discharges from three different batches of microgels (n=3).

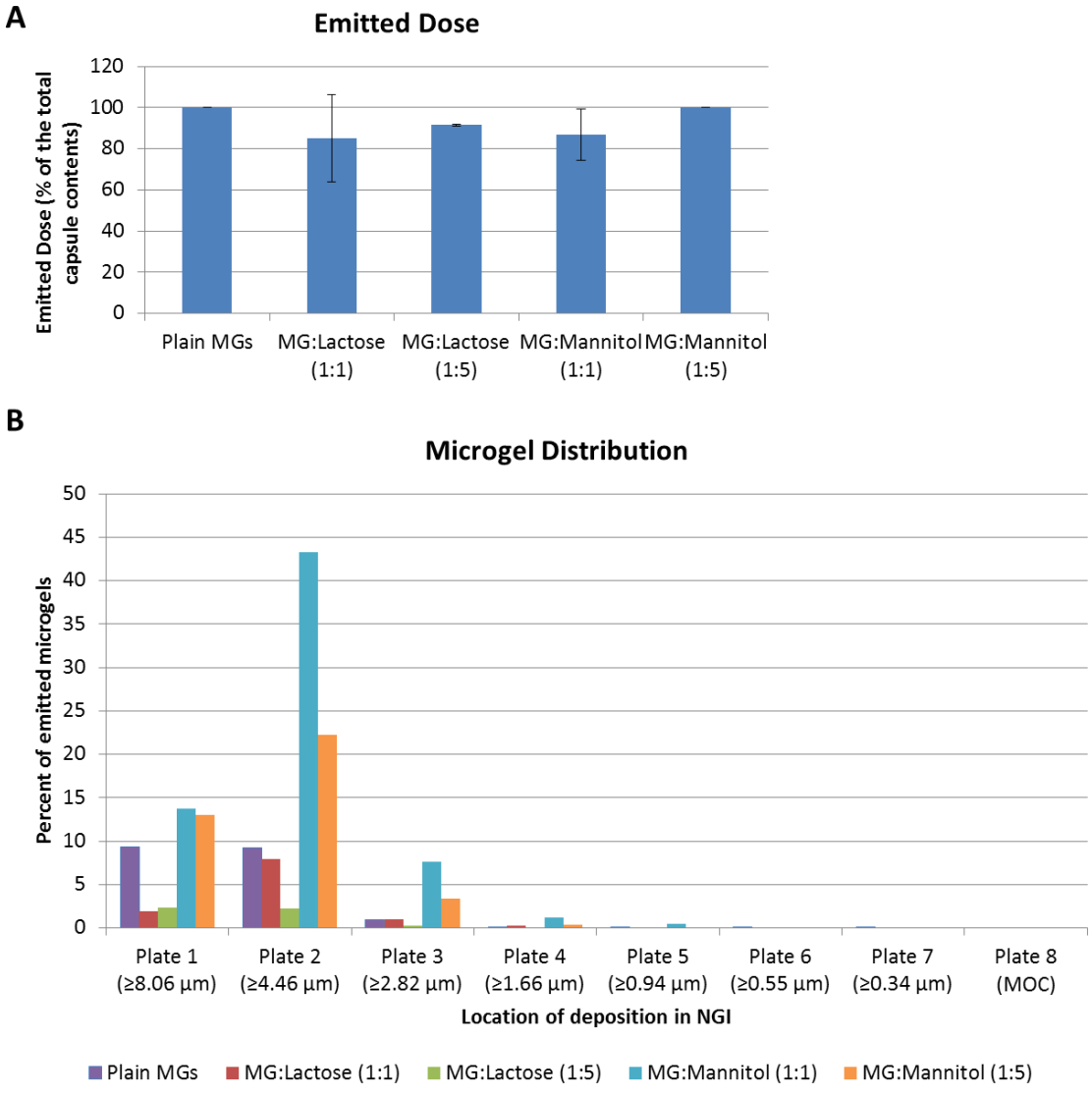

Figure 2.8 Formulation development 2: DPI emitted dose and microgel NGI distribution

The microgels were lyophilized with inhalation grade lactose then loaded into HPMC size 3 capsules, actuated within the DPI device, and deposited within the NGI at a flow rate of 60 L/min for 4 seconds. Each NGI run consisted of three microgel-loaded capsule discharges from three different batches of microgels (n=3).

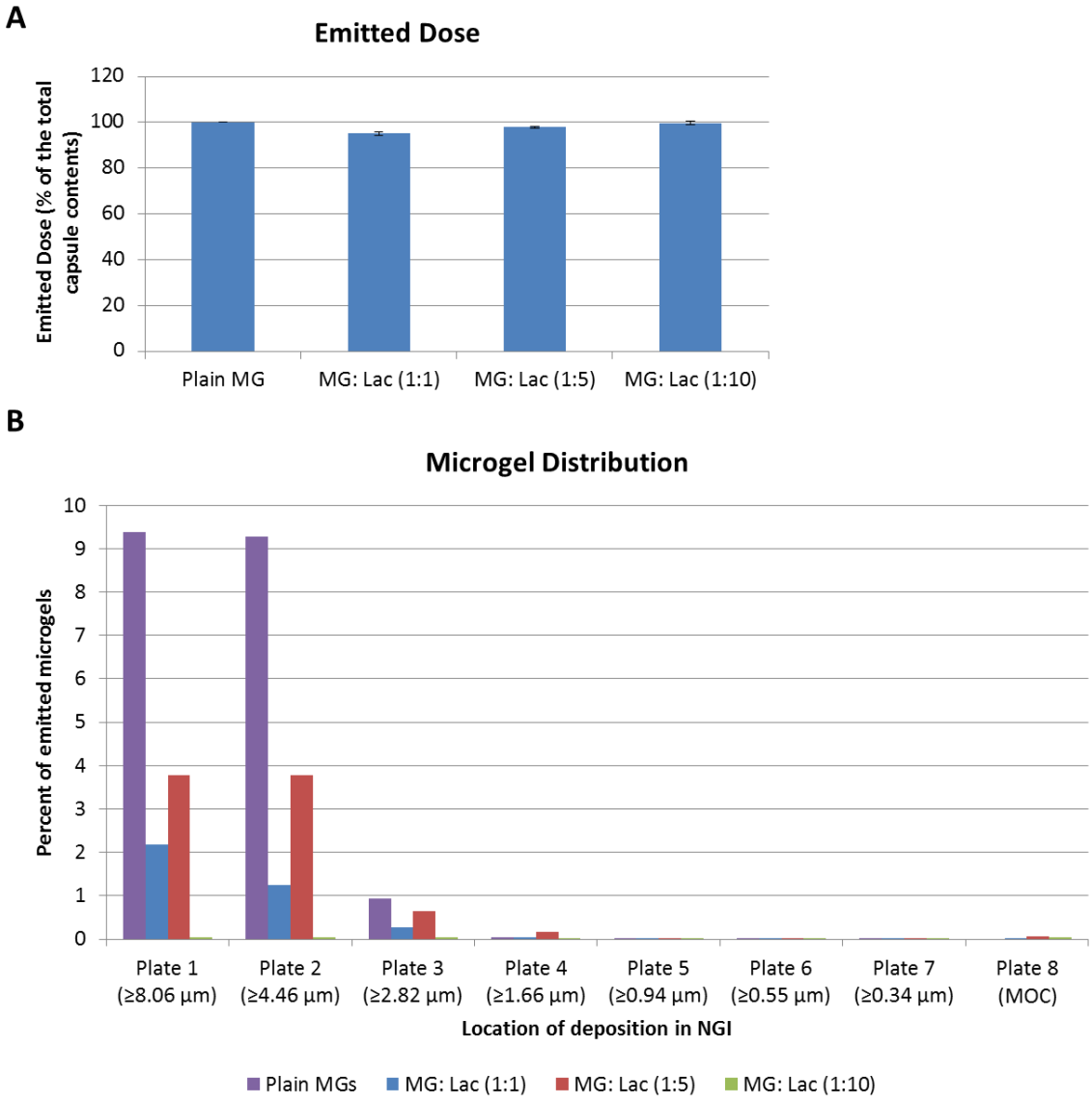

Figure 2.9 Formulation development 3: DPI emitted dose and microgel NGI distribution

The microgels were lyophilized with inhalation grade lactose then blended in Turbula blender for 30 minutes before being loaded into HPMC size 3 capsules, actuated within the DPI device, and deposited within the NGI at a flow rate of 60 L/min for 4 seconds. Each NGI run consisted of three microgel-loaded capsule discharges from three different batches of microgels (n=3).

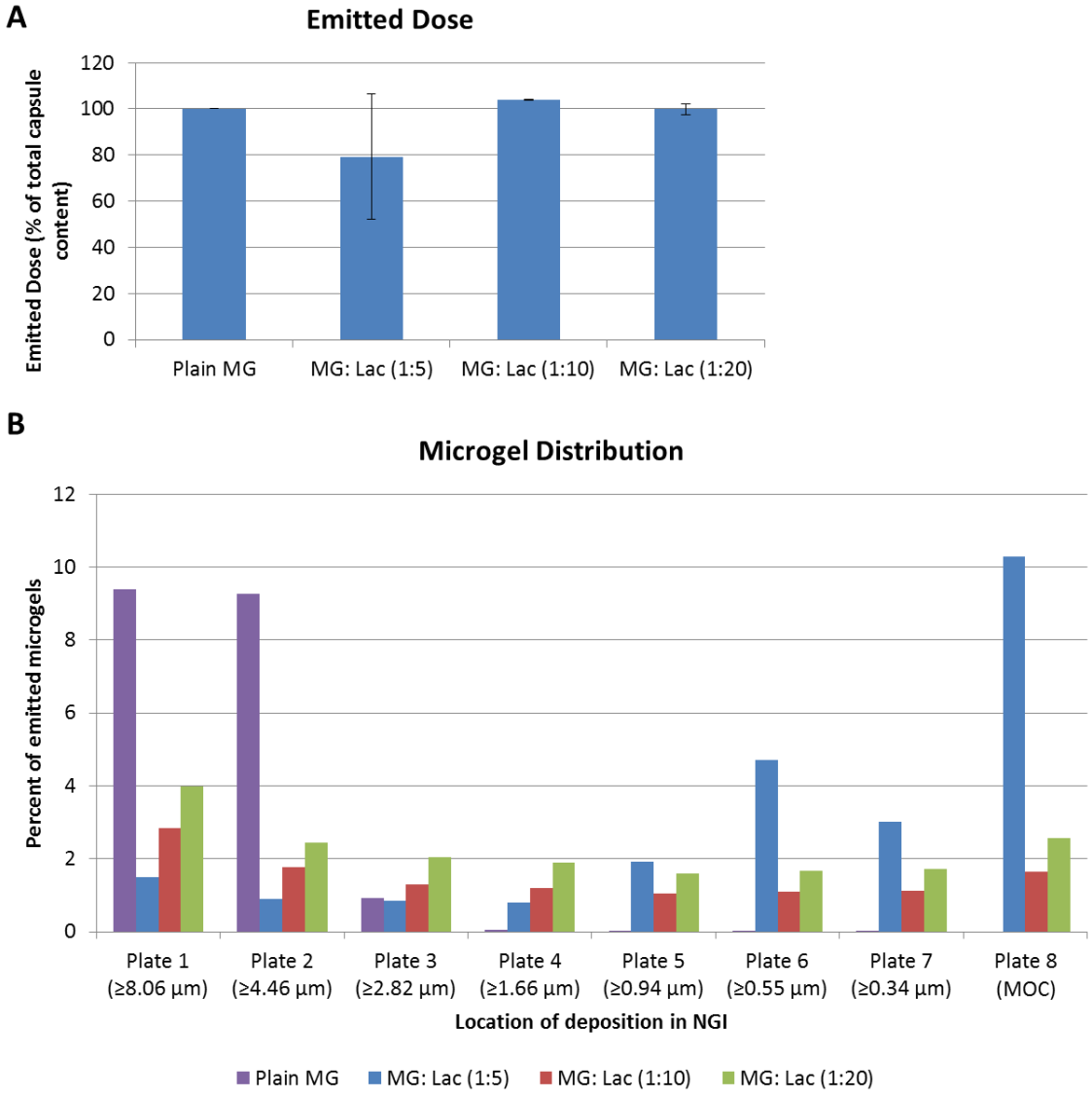

Figure 2.10 Percent of microgels remaining in lungs over time

Microgels were delivered to mouse lungs via intratracheal administration. The percent of microgels remaining in the lungs over time was measured by fluorescence quantification from lung tissue homogenates.

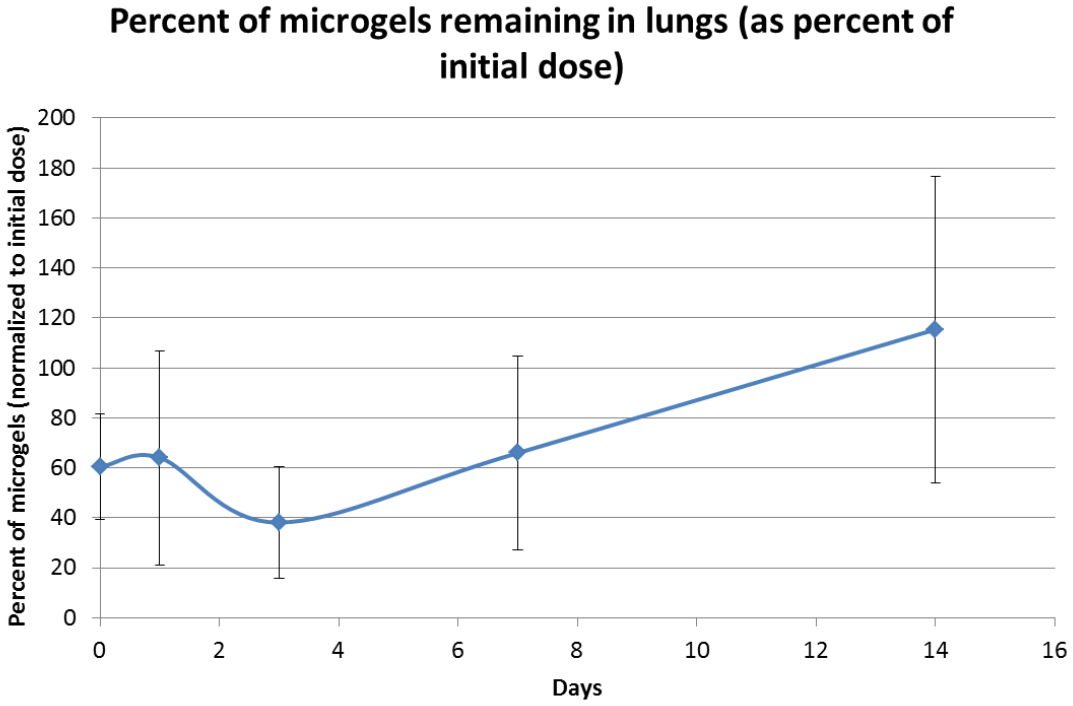

2.4 REFERENCES

[1] L. Brannon-Peppas, “Preparation and Characterization of Crosslinked Hydrophilic Networks,” in *Studies in Polymer Science*, vol. Volume 8, Lisa Brannon-Peppas and Ronald S. Harland, Ed. Elsevier, 1990, pp. 45–66.

[2] N. A. Peppas, P. Bures, W. Leobandung, and H. Ichikawa, “Hydrogels in pharmaceutical formulations,” *Eur. J. Pharm. Biopharm.*, vol. 50, no. 1, pp. 27–46, Jul. 2000.

[3] N. A. Peppas, B. V. Slaughter, and M. A. Kanzelberger, “9.20 - Hydrogels,” in *Polymer Science: A Comprehensive Reference*, Editors-in-Chief: Krzysztof Matyjaszewski and Martin Möller, Eds. Amsterdam: Elsevier, 2012, pp. 385–395.

[4] I. M. El-Sherbiny, S. McGill, and H. D. C. Smyth, “Swellable microparticles as carriers for sustained pulmonary drug delivery,” *J. Pharm. Sci.*, vol. 99, no. 5, pp. 2343–2356, May 2010.

[5] P. Wanakule, G. W. Liu, A. T. Fleury, and K. Roy, “Nano-inside-micro: Disease-responsive microgels with encapsulated nanoparticles for intracellular drug delivery to the deep lung,” *J. Controlled Release*, vol. 162, no. 2, pp. 429–437, Sep. 2012.

[6] D. A. Edwards and C. Dunbar, “BIOENGINEERING OF THERAPEUTIC AEROSOLS,” *Annu. Rev. Biomed. Eng.*, vol. 4, no. 1, pp. 93–107, Aug. 2002.

[7] S. Stegemann, S. Kopp, G. Borchard, V. P. Shah, S. Senel, R. Dubey, N. Urbanetz, M. Cittero, A. Schoubben, C. Hippchen, D. Cade, A. Fuglsang, J. Morais, L. Borgström, F. Farshi, K.-H. Seyfang, R. Hermann, A. van de Putte, I. Klebovich, and A.

Hincal, “Developing and advancing dry powder inhalation towards enhanced therapeutics,” *Eur. J. Pharm. Sci.*, vol. 48, no. 1–2, pp. 181–194, Jan. 2013.

[8] C. Evora, I. Soriano, R. A. Rogers, K. M. Shakesheff, J. Hanes, and R. Langer, “Relating the phagocytosis of microparticles by alveolar macrophages to surface chemistry: the effect of 1,2-dipalmitoylphosphatidylcholine,” *J. Controlled Release*, vol. 51, no. 2–3, pp. 143–152, Feb. 1998.

[9] M. Bhavsar and M. Amiji, “Development of Novel Biodegradable Polymeric Nanoparticles-in-Microsphere Formulation for Local Plasmid DNA Delivery in the Gastrointestinal Tract,” *AAPS PharmSciTech*, vol. 9, no. 1, pp. 288–294, Mar. 2008.

[10] M. P. Lutolf and J. A. Hubbell, “Synthesis and Physicochemical Characterization of End-Linked Poly(ethylene glycol)-co-peptide Hydrogels Formed by Michael-Type Addition,” *Biomacromolecules*, vol. 4, no. 3, pp. 713–722, Feb. 2003.

[11] M. Irngartinger, V. Camuglia, M. Damm, J. Goede, and H. . Frijlink, “Pulmonary delivery of therapeutic peptides via dry powder inhalation: effects of micronisation and manufacturing,” *Eur. J. Pharm. Biopharm.*, vol. 58, no. 1, pp. 7–14, Jul. 2004.

[12] C.-C. Lin and A. T. Metters, “Hydrogels in controlled release formulations: Network design and mathematical modeling,” *Comput. Drug Deliv.*, vol. 58, no. 12–13, pp. 1379–1408, Nov. 2006.

[13] J. Zhang, A. Skardal, and G. D. Prestwich, “Engineered extracellular matrices with cleavable crosslinkers for cell expansion and easy cell recovery,” *Biomaterials*, vol. 29, no. 34, pp. 4521–4531, Dec. 2008.

[14] M. R. Preiss, “Stimuli-responsive liposome-nanoparticle assemblies,” *Expert Opin. Drug Deliv.*, vol. 8, no. 8, pp. 1025–40, 2011.

[15] E. Fleige, M. A. Quadir, and R. Haag, “Stimuli-responsive polymeric nanocarriers for the controlled transport of active compounds: Concepts and applications,” *Approaches Drug Deliv. Based Princ. Supramol. Chem.*, vol. 64, no. 9, pp. 866–884, Jun. 2012.

[16] M. Ehrbar, S. C. Rizzi, R. G. Schoenmakers, B. San Miguel, J. A. Hubbell, F. E. Weber, and M. P. Lutolf, “Biomolecular Hydrogels Formed and Degraded via Site-Specific Enzymatic Reactions,” *Biomacromolecules*, vol. 8, no. 10, pp. 3000–3007, Sep. 2007.

[17] F. Ahsan, I. P. Rivas, M. A. Khan, and A. I. Torres Suárez, “Targeting to macrophages: role of physicochemical properties of particulate carriers—liposomes and microspheres—on the phagocytosis by macrophages,” *J. Controlled Release*, vol. 79, no. 1–3, pp. 29–40, Feb. 2002.

[18] G. Pilcer and K. Amighi, “Formulation strategy and use of excipients in pulmonary drug delivery,” *Int. J. Pharm.*, vol. 392, no. 1–2, pp. 1–19, Jun. 2010.

[19] W. Abdelwahed, G. Degobert, S. Stainmesse, and H. Fessi, “Freeze-drying of nanoparticles: Formulation, process and storage considerations,” *2006 Suppl. Non-Themat. Collect.*, vol. 58, no. 15, pp. 1688–1713, Dec. 2006.

[20] W. Abdelwahed, G. Degobert, and H. Fessi, “Investigation of nanocapsules stabilization by amorphous excipients during freeze-drying and storage,” *Eur. J. Pharm. Biopharm.*, vol. 63, no. 2, pp. 87–94, Jun. 2006.

[21] Y. N. Konan, R. Gurny, and E. Allémann, “Preparation and characterization of sterile and freeze-dried sub-200 nm nanoparticles,” *Int. J. Pharm.*, vol. 233, no. 1–2, pp. 239–252, Feb. 2002.

[22] A. Saez, M. Guzmán, J. Molpeceres, and M. . Aberturas, “Freeze-drying of polycaprolactone and poly(d,l-lactic-glycolic) nanoparticles induce minor particle size changes affecting the oral pharmacokinetics of loaded drugs,” *Eur. J. Pharm. Biopharm.*, vol. 50, no. 3, pp. 379–387, Nov. 2000.

[23] C. Schwarz and W. Mehnert, “Freeze-drying of drug-free and drug-loaded solid lipid nanoparticles (SLN),” *Int. J. Pharm.*, vol. 157, no. 2, pp. 171–179, Nov. 1997.

[24] B. Patel, V. Gupta, and F. Ahsan, “PEG–PLGA based large porous particles for pulmonary delivery of a highly soluble drug, low molecular weight heparin,” *J. Controlled Release*, vol. 162, no. 2, pp. 310–320, Sep. 2012.

[25] K. Hirose, A. Marui, Y. Arai, T. Kushibiki, Y. Kimura, H. Sakaguchi, H. Yuang, B. I. R. S. Chandra, T. Ikeda, S. Amano, Y. Tabata, and M. Komeda, “Novel approach with intratracheal administration of microgelatin hydrogel microspheres incorporating basic fibroblast growth factor for rescue of rats with monocrotaline-induced pulmonary hypertension,” *J. Thorac. Cardiovasc. Surg.*, vol. 136, no. 5, pp. 1250–1256, Nov. 2008.

[26] A. Pusztai, “Both free and complexed trypsin inhibitors stimulate pancreatic secretion and change duodenal enzyme levels,” *Am. J. Physiol.*, vol. 272, no. 2, pp. G340–50, 1997.

Chapter 3: Hydrogel Encapsulating Stem Cells for *In Vitro* T Cell Differentiation

3.1 Background and Significance

Hydrogels offer a unique 3D environment for cells. By encapsulating cells within hydrogel systems we can enhance cell-cell and cell-material interactions that differ from 2D systems. Using 3D environments allows us to create more biomimetic reconstructions of the cell's natural surrounding within tissue. It also gives us the tools to fine tune factors such as cell density, ligand density, and mechanical properties of the hydrogel in order to promote cell growth and differentiation in the case of stem cells. The systems can also promote maintenance of physiological cellular morphologies.

3.1.1. Motivation

T cells are key players in the body's inherent disease-fighting strategy. Many treatments for diseases such as melanoma, renal cancer, multiple myeloma, prostate cancer, leukemia, nasopharyngeal cancer, Hodgkin's disease, and post-transplant lymphoproliferative diseases rely on immunotherapy with autologous T cells [1]–[4]. Currently, successful *ex vivo* immunotherapy with autologous T cells is performed by adoptive transfer, a therapy where T cells are isolated from the patient's peripheral blood, expanded *ex vivo*, trained or selected for antigen specificity, expanded further, then transplanted back into the patient [5]. Although adoptive transfer of T cells for treatment of certain cancers has been successful there are significant disadvantages to the method. There is often limited availability of donor cells (autologous or allogeneic) and the patient cell isolation can be highly inefficient and lead to potential complications for the patient. There are considerable costs and lengthy time requirements necessary for adoptive therapy which is not conducive for patients with advanced diseases or in need of an "on demand" source of T cells [6], [7]. There is a clear need for large scale, efficient

production of antigen-specific T cells for on-demand therapy. It is hypothesized that stem cells can offer a suitable source for adoptive transfer cells through *in vitro* T cell differentiation.

3.1.2 T Cell Development

In order to induce T cell differentiation of stem cells, a thorough understanding of physiological T cell development must be understood. Most blood cells develop and mature in the bone marrow; however, T cell development occurs in the thymus where hematopoietic progenitor cells undergo development and selection while travelling through distinct regions of the thymus [8]. T cells and B cells are of the same lymphoid lineage, T cells called thus because of "T" for thymus and B cells called "B" for bone marrow. To mimic the development of T cells *in vitro* we assess the natural thymic niche and the necessary soluble and insoluble signals it provides for T cell development *in vivo*.

The thymus, located in front of the heart and behind the sternum, can be divided into the cortex and the medulla. T cells travel through the cortex and the medulla going through stages of development. During this process there are two key signals presented in the thymic niche in sequence that are necessary for the development of T cells: signaling between Delta like ligands and Notch receptor and signaling between Major Histocompatibility Complex and T cell receptor [9], [10]. The first stages for developing T cells are called the double negative (DN) stages where the cells transition sequentially through DN1, DN2, DN3, and DN4 stages while traveling from the cortico-medullary junction through the outer cortex to the subcapsular zone of the thymus. These stages differ in the expression of surface markers CD44 and CD25. The next stage differentiation is the transition from double negative (DN) to double positive (DP) stage where the T cells present surface markers CD4 and CD8. Notch signaling, the first key

signal required for differentiation, is responsible for the transition of T cells from DN1 to DN2. Other factors needed for the differentiation include cytokines stem cell factor (SCF) and interleukin (IL-7). During the DN3 stage the T cells experience T cell receptor (TCR) β rearrangement and β-selection and eventually the cells undergo αβ TCR expression and become DP cells. The next phase of development is positive selection. Positive selection is induced by major histocompatibility complexes (MHC) class I and class II molecules presented on cortical epithelial/stromal cells. These MHC molecules are associated with self-peptides that induce the differentiation of DP thymoctyes into single positive (SP) thymocytes. SP stage cells express either CD4 or CD8 expression markers, identifying them as either helper T cells or cytotoxic T cells respectively. The T cells then travel through the cortico-medullary junctions into the medulla. The next step is negative selection where the thymocytes that experience strong affinity for self peptide-MHC complexes and pose possible auto-immunity are eliminated. The result of the differentiation and development pathway through the thymus are mature self-tolerant T cells that are now capable of defending the body in an immune response [8], [10], [11].

3.1.3 Delta Like Ligands and Notch Receptor Signaling

As mentioned previously, the Notch signaling in the thymic niche is essential in generation functional T cells. Schmitt and Zúñiga-Pflücker demonstrated that providing Notch signaling to a system previously designed for B cell development from hematopoietic progenitor cells resulted in T cell maturation [12]. In addition to hematopoietic and T cell differentiation, notch signaling occurs during many stages of embryonic development and in adult self-renewal systems including neuronal, cardiovascular, and myogenesis development stages. It is considered an evolutionarily conserved pathway. Four mammalian Notch receptors (Notch 1-4) have been identified,

all of which are transmembrane proteins that bind to cell surface ligands belonging to either the Delta or Jagged/Serrate family [13].

During T cell development in the thymus, it has been determined that Notch1 is involved in binding with Delta-like ligands DLL1 and DLL4 during the early stages of T cell development while inhibiting B cell differentiation [14], [15]. The ligand binding induces a proteolytic cleavage within the Notch intracellular domain. Ultimately, the intracellular Notch domain (ICN) translocates into the nucleus and binds to DNA-binding CSL(RBPJκ) protein to activate target genes that are generally responsible for Notch functions that require inhibition of one specific cell fate to allow determination of an alternative fate [16].

DLL1 and DLL4 share a high degree of homology and have been shown to induce T cell differentiation *in vitro*. However, DLL4 appears indispensable *in vivo* while DLL1 is not. Unlike DLL1 inactivation, DLL4 inactivation in thymic epithelial cells results in a complete block of T cell development [4,5,6]. Mohtashami et al. from Zúñiga-Pflücker group noted that DLL4-expressing stromal cells induced greater activation of downstream Notch genes and higher T cell differentiation than DLL1-expressing stromal cells [20]. Reasoning to the more effective T cell differentiation caused by DLL4 is attributed to greater avidity in DLL4 binding to immature thymocytes, higher rates of endocytosis, and more effective binding activation and cleavage of Notch receptor [20]. It has also been shown by Dallas et al. from the Bernstein group that notch signaling is dose dependent and lower densities support B cell generation while higher densities support T cell generation [21].

3.1.4 Strategies for *In Vitro* T Cell Differentiation

Although simple techniques for B cell development have been established *in vitro* [22], [23], the generation of T cells has proved to be more difficult and complex. Up until the 1990s the only *in vitro* system established for the successful differentiation of T cells was the cumbersome fetal thymic organ culture (FTOC) [24]. FTOC allowed for the differentiation of hematopoietic stem cells into T cells in isolation, however the system it was difficult to quantitatively characterize or control the signaling and the whole process was very time consuming, expensive, and inefficient [25].

Subsequent studies focusing on the development of hematopoietic stem cells emphasized the role of Notch signals in the development of T and B cells. In 1999 Radtke et al. used Notch-1 knockout mice to show that Notch-1-deficient hematopoietic progenitor cells developed into B cells in the thymus rather than T cells [26]. Additionally, Pui et al. showed that bone marrow cells transduced with NotchIC failed to differentiate into B cells *in vivo* and induced double positive T cells [27]. Schmitt and Zúñiga-Pflücker transduced the bone marrow stromal cell line OP9 to ectopically express DLL1 [12]. Previously, the OP9 cell line supported B cell development from HSCs, however the new OP9-DL1 cells in co-culture with HSCs induced T cell development.

Stroma-free approaches off the advantage of avoiding the contamination of stromal cells, such as the OP9-DL1 cell line created from bone marrow stromal cells transfected to present immobilized Notch ligand DLL1. In 2000, Varnum-Finney et al. demonstrated that immobilization of DLL1 on plastic surfaces was required to activate Notch signaling in C2 myoblasts and U20S cells [28]. Further immobilized DLL1 in combination with a cocktail of cytokines could support mouse bone marrow HPC expansion and further T cell lineage commitment [29]. Kotov and colleagues have also shown the possibly of early T cell differentiation from human HSCs through 3D inverted

colloidal crystal scaffolds coated with DLL1 [30]. Studies up to this point have successfully used DLL1-coated surfaces for Notch signaling in HPCs to show differentiation up to early T cells but have yet to produce a system for the complete differentiation of HPCs into functional mature DP or SP T cells. Additionally, the majorities of the findings are limited to 2D cultures and have not ventured into 3D biomaterial environments.

3.1.5 Hydrogel Design for 3D Microenvironment

A biomaterials based approach to T cell differentiation will offer the ability to mimic the biological environment of the thymus. Mimicking the thymic niche *in vitro* requires consideration of multiple components. Essentially, the thymic niche includes epithelial cells which provide Notch ligands and receptors, T cell receptors, and MHC molecules [31]. Additionally, there are soluble factors present including IL-7, SCF, and various chemokines [11]. Lastly, the extracellular matrix is present and composed of laminin, collagen, and fibronectin [32]. A comprehensive understanding of the microenvironments of cells can further our ability to direct the development of T cells *in vitro*. Many of the culture systems for developing functional T cells are limited to 2D surfaces. These culture systems ignore the natural cellular environment that our cells develop within our body and organs. 3D biomaterials can offer comparable mechanical surfaces of the thymic microenvironment, increased ligand presentation, and increased cell-cell and cell-matrix interactions, as well as the dynamic culture system better resembling tissue microenvironments.

Studies more recently have reported that stem cell fate and lineage specification can be directed by substrate mechanical and biochemical properties [33]. PEG based biomaterials have been widely used in studies because of biocompatibility, fabrication

ease, and tunable mechanical properties. It is accepted that mechanical properties of the substrate play a role in cell behavior [33]–[35]. Substrate stiffness affects cell adhesion, contractility, motility, and cell fate [36]. Engler et al. reported that naïve mesenchymal stems cells commited to lineage specified by matrix elasticity in culture [34]. Holst et al. inferred through studies that murine and human HSCs respond directly to biomechanical forces [37]. It has also been reported that substrate elasticity was influential in mature T cells [38].

Apart from mimicking the thymic microenvironment, 3D biomaterials offer the potential for a stroma-free approach to *in vitro* T cell development. By engineering biomaterials to present Notch ligands immobilized on surfaces, the cultures can avoid the contamination of animal ligand presenting stromal cells. Lutolf et al. assessed the effects of secreted and tethered proteins characteristic of *in vivo* microenvironment on HCS fate through poly(ethylene glycol), PEG, hydrogel microwell arrays. The studies showed that signaling proteins could be presenting to HSCs and validated the PEG based biomaterial system as a viable system to mimic the complex stem cell niche [39]. Ligand immobilization has been studied by the Bernstein group with successful differentiation into early T cells [21].

The design adapted in this report for *in vitro* T cell differentiation uses PEG and HA based hydrogels to mimic the microenvironment of the thymic niche for HSCs, embryonic stem cells, and induced pluripotent stem cells. Hydrogels are crosslinked polymer networks that resemble physical characteristics to soft tissue, making them ideal for tissue engineering purposes [40]. PEG has been widely used in mechanobiological studies because of its ease of fabrication, biocompatibility, and easily tunable mechanical stiffness. Lutolf et al. used a PEG hydrogel microwell system to create artificial niches to study the regulatory role of specific signals on single HSC fates [39].

The hydrogel polymer complex in this report also utilizes the benefits of hyaluronic acid (HA). HA is a linear, negatively charged, high molecular weight, and acidic glycosaminoglycan (GAG) composed of D-glucaronic acid β-1 and 3-N-acetylglucosamine-β-1,4 [41]–[43]. HA is distributed through the body's ECM and plays significant roles in tissue repair, cell migration, cell proliferation, and cell differentiation. One source of HA in the body includes stromal cells and forms a major component of the bone marrow extracellular matrix [41]. Because HA and its derivatives are biocompatible and biodegradable, they are widely used in tissue engineering and medicine. Gerecht et al. reported the use of HA hydrogels to support controlled long-term self-renewal of human embryonic stem cells in the presence of conditioned medium. Also, when encapsulated in HA hydrogels differentiation was induced by altering soluble factors [44].

The hydrogels were formed by a crosslinking strategy developed by the Prestwich group [45] and the majority of components were purchased through Glycosan BioSystems (BioTime, Inc). The gels are synthesized via disulfide crosslinking of thiolated HA derivatives (Carboxymethyl Hyaluronic Acid - DTPH, M_w 158kDa) and the thiol-reactive crosslinker PEG-diacrylate (PEGDA, M_w 3400kDa) [46], [47]. The crosslinking between acrylate groups and thiols is the same chemistry of a conjugate addition reaction. The hydrogels support cell viability and the majority of cells survive crosslinking [47]. Additionally, gelatin was incorporated for some studies reported here to determine the effect of cell attachment on differentiation within the hydrogels. The gelatin component (Carboxyxmethyl Gelatin-DTPH), also reported by the Prestwich group, was thiol-modified to crosslink with PEGDA [46]. In order to release the cells after periods of encapsulation, it is necessary to degrade the hydrogel without infflicting cell death. Degradation was performed in two different manners. For the hydrogels with

PEGDA, the gels were enzymatically degraded with hyaluronidase (HAse). However, because the enzymatic degradation can potentially damage sensitive cells, PEGSSDA was used in some of the studies in this report instead of PEGDA. PEGSSDA is a pentablock PEGDA molecule composed of four PEG molecules and two interdigitated disulfide bonds. PEGSSDA is still a thiol-reactive crosslinker that covalently reacts with the thiol groups of the modified HA and gelatin. Incorporation of PEGSSDA into the hydrogels allows for degradation via dissolution of the disulfide bond of PEGSSDA through a thiol-disulfide exchange reaction [48]. For stroma free approaches, this report used the incorporation of biotylinated Delta like ligands and microbeads with surface immobilized Delta-like ligands within the hydrogels.

3.2 Materials and Methods

3.2.1 Hydrogel Synthesis and Characterization

3.2.1.1 Hydrogel synthesis

Protocol for synthesis of HA-PEG hydrogels was adapted from Glycosan Biosystems (BioTime, Inc, Alameda, CA) where components were purchased. The HA (Carboxymethyl Hyaluronic Acid - DTPH, M_w 158kDa) and gelatin (Carboxyxmethyl Gelatin-DTPH) components purchased from Glycosan were dissolved separately in 1mL of degassed water for a concentration each of 1% (w/v). The solutions were placed on a rocker and incubated at 37°C for 20 minutes to allow for sufficient time for the solid to dissolve. For cell encapsulation, cells were resuspended directly to the HA solution after this step at the desired concentration. The PEG component of the hydrogel was dissolved in 0.5 mL or 0.25 mL depended on the desired crosslinking wanted for the hydrogels, either a 2% (w/v) or 4% (w/v) concentration. For hydrogels with gelatin, 100 µL of gelatin solution was combined to 100 µL of HA and cell, then 50 µL of PEG component

added. To form the hydrogels without gelatin, the 50 μL of the PEG solution was added to 200 μL of HA and cell solution for a volume ratio of 1:4. The gels were mixed before complete gelation by pipetting to ensure cells were evenly dispersed. After 20 minutes of gelation within an incubator, media was added.

3.2.1.2 Hydrogel degradation and dissolution

For hydrogels composed of PEGSSSDA, dissolution of gels was performed with 40mM N-Acetyl-L-Cysteine (Sigma-Aldrich, St. Louis, MO) in sterile 1X PBS. The solution pH was adjusted to between 7.3 and 7.5 and filtered. To dissolve the gels, media was removed and 1 mL of N-Acetyl-L-Cysteine added. Every 10-20 minutes, the gels and solution were mixed by pipetting to speed the dissolution process. Once the gels were completely dissolved, the suspension was centrifuged to obtain the cell pellet.

For hydrogels without PEGSSDA, and composed for PEGDA with HA, and possibly gelatin, hyaluronidase (HAse) (Sigma-Aldrich, St. Louis, MO) was used for degradation. Hyaluronidase from bovine testes, Type IV-S and mouse embryo tested, was purchased from Sigma-Aldrich and used at a concentration of 10% w/v in PBS to degrade the hydrogels. Between 0.5 and 1 mL of HAse solution was added to the gels. Every 10-20 minutes, the gels and solution were mixed by pipetting to speed the dissolution process. Once the gels were completely dissolved, the suspension was centrifuged to obtain the cell pellet.

3.2.1.3 Rheology testing

In order to better mimic the thymic niche, the material properties of the hydrogel were compared to that of the mouse thymus. The mechanical properties were tested using a rheometer (Anton Paar Physica MCR 101) utilizing a 7.974 mm diameter oscillatory measuring system. To choose proper frequency and strains for testing, frequency and

strain sweep measurements were initially performed on the gels and the appropriate values were determined based on linear regions in the sweeps. These linear regions represent the best frequency and strain to use for accurate measurements. The measurements were chosen to be taken at a frequency of 1 Hz and 5% strain. Gap sizes were chosen to approximately equalize initial compression across all gels and thymuses. Hydrogels were prepared in 8 mm silicone isolator molds and undergone an initial swelling period before being transferred to rheometer for storage modulus measurements. Bulk thymus lobes were obtained from female BALB/c mice (Jackson Laboratories, Bar Harbor, ME) ranging in age from 4 to 8 weeks. It was assumed that the bulk rheological measurements for the thymus are comparable to the mechanical properties of what the thymocytes experience in the thymic epithelial cells. The storage modulus was used as a mechanical property to compare across samples.

3.2.2 Cell Isolation and Encapsulation

3.2.2.1 Mouse bone marrow hematopoietic progenitor cell isolation and culture

Primary mouse hematopoietic progenitor cells were obtained from bone marrow of 4 to 6 week old female BALB/c mice (Jackson Laboratories, Bar Harbor, ME). The mice were sacrificed by primary method of euthanasia by CO_2 then secondary method of cervical dislocation. The legs of the mice were removed from above the hip joint using scissors. Then the skin down to the foot was removed using forceps, scissors, and Kimwipes. The foot was then removed and the femur and tibia separated. The bone was exposed by removing all the tissue surrounding it. The femur and tibia were sterilized by soaking for one minute in 70% ethanol. The bone marrow was obtained by a flushing method where the femur and tibia were cut at the top and the bottom, exposing the bone marrow. Using a 21 gauge needle-loaded syringe, PBS was flushed through the bone to

rinse out all the bone marrow. After the bone marrow had been collected, it was resuspended using a 16 gauge needle in order to break up and remove any clumps within the suspension.

After isolation of bone marrow, the cell suspension was centrifuged and 1X Red Blood Cell Lysis Buffer (eBioscience, San Diego, CA) was added to the cell pellet for ten minutes. The following steps were performed to ensure that only lineage negative (Lin-) cells were isolated for experiments. The lineage positive cells, indicating mature hematopoietic cells, such as developed T cells, B cells, monocytes, macrophages, granulocytes, and erythrocytes were depleted from the suspension using magnetic separation with the Lineage Depletion Kit (Miltenyi Biotec, Bergisch Gladbach, Germany). First, magnetic microbeads modified to preset antibodies for various lineage markers, such as CD5, CD45R(B220),CD11b, Anti-Gr-1(Ly-6G/C),and Ter-119, were added to the bone marrow cells. After incubating with the microbeads briefly, the cells were passed through a magnetic column (MACS® LS Cell Separation Columns, MiniMACS^{TM} Separator, Mitenyi Biotec). The lineage positive cells, bound to the magnetic microbeads, were separated from unbound lineage negative cells that were able to freely pass through the column. The lineage negative bone marrow cells were then stained with anti-mouse c-Kit APC and anti-mouse sca-1 PE antibodies (eBioscience). The cells were incubated with the antibodies then washed with cell buffer twice before being sorted by fluorescence activated cell sorting (FACS) on BD FACS Aria II (Beckton Dickinson, Franklin Lakes, NJ) at the Dell Pediatric Research Institute Flow Cytometry Core Facility (Austin, Texas). The cells were sorted for c-Kit positive and sca-1 positive, thereby obtaining a final population of Lin-c-Kit+sca1+ cells.

The cells were then directly encapsulated into hydrogels at a concentration of 5,000 cells, as described below, or seeded onto tissue culture wells plates, possibly

containing an 80% confluent OP9-DL1 monolayer. The cells were cultured in OP9 Media of 20% Defined FBS, 1% pen/strept, and 89% alpha MEM with 5ng/mL human Flt-3L and 1 ng/mL murine Il-7.

3.2.2.2 Mouse embryonic stem cell culture and expansion

Murine embryonic stem cells (R1, Nagy Lab) or murine pluripotent stem (iPS) cells (iPS-MEF-Ng-20D-17, Riken Cell Bank) were expanded on mouse embryonic fibroblast (MEF) feeder layers. The MEF cells were seeded onto two gelatin-coated T-25 tissue culture flasks as a concentration of 5 x 10^5 cells per flask. Once one T-25 flask reached approximately 80% confluency, it was inactivated with 10 µg/mL of mytomycin C solution in DMEM with 5% embryonic stem cell screened defined Fetal Bovine Serum (ES-screened FBS, StemCell Technologies, Vancouver, BC) for 3 hours at then rinsed with sterile PBS and replaced with MEF growth medium. The second flask was passaged, 1:6, into two gelatin-coated T-75 tissue culture flasks which were also inactivated at approx. 80% confluency. The stem cells were then expanded on top of the MEF feeder layer and cultured to methods described by Taqvi et al. [49].

3.2.3 Cell Flow Cytometry Analysis

At the specified time points for analysis, cells were isolated and prepared for flow cytometry analysis to determine the presence of cell surface markers indicating stages of differentiation. Cells were suspended in FACS buffer consisting of sterile PBS with 2% (w/v) ES-screened FBS, 0.1% (w/v) NaN_3, and 2mM EDTA. Anti-mouse CD16/CD32 Fc Block (BD Pharmingen, San Jose, CA) was added to the cells for 10 minutes to prevent any unspecific binding of antibodies on cell. Cells were then incubated for 30 minutes at 4°C with pre-determined antibodies from the following: anti-Thy1.2, anti-CD19, anti-CD25, anti-CD44, anti-CD4, anti-CD8, and 7-AAD (eBioscience). The 7-AAD stain was

used to gate out the dead cell population and analyze only living cells. An isotype control (eBioscience) was prepared for each stain for a negative control. The cell suspension was then washed twice in FACS buffer by resuspension followed by centrifugation and removal of supernatant containing unbound antibodies. Flow cytometry was performed on either BD FACS Aria II (Beckton Dickinson) or on BD Accuri (Beckton Dickinson). The data was then gated for cell populations expressing surface markers and analyzed using FlowJo software (Tree Star).

3.2.4 Ligand Incorporation

Mouse delta like ligand 4 (DLL4) (R&D Systems, Minneapolis, MN) was biotinylated in order to immobilize on streptavidin modified surfaces and biomaterials. Biotin-XX-succinimidyl ester (Biotin-XX Microscale Protein Labeling Kit, Life Technologies) was conjugated to DLL4 in sodium bicarbonate buffer for 15 minutes. Any unconjugated biotin and residue was removed by resin filtration in a centrifugal filter. For certain studies, biotinylated bovine serum albumin tagged with fluorescein (biotin-BSA-FITC) (Nanocs) was used as a model bDLL4.

Streptavidin was conjugated to PEG acrylate to incorporate streptavidin into the hydrogel network and bind bDLL4. Streptavidin (Promega, Madison, WI) with molecule weight of 66kDa and 15 units/mg was dissolved in 50nM $NaHCO_3$ buffer at a concentration of 1mg per 100uL. PEGDA was added to the solution at a molar ratio of 1:10 of streptavidin to PEG. After rotating for 2 hours, the solution was washed in deionized water twice to obtain the final PEGylated streptavidin (strept-PEG-acryl).

3.2.5 DLL4 Coated Magnetic Microbeads

Cobalt-based magnetic microbeads from the Dynabeads® His-Tag Isolation Pulldown Kit (Life Technolgies) were used to specifically bind his-tagged Delta like

ligand 4 (Sino Biologicals, Beijing, China). The 6 million beads with 1.1 μm diameters were mixed with 12 μg of his-tagged protein in PBS. The suspension was placed on a rotating shaker for 30 minutes to allow for binding of protein to bead before washing three times with a magnet (DynaMag^{TM}, Life Technologies) to remove all unbound DLL4.

3.3 Results and Discussion

3.3.1 Hydrogel Characterization

The hydrgogel characterization studies, such as swelling, degradation, and cell viability, were extensively studied and published by previous research groups [46]–[48]. Cell viability studies were confirmed as well as dissolution studies. **Figure 3.1** shows light microscopy images of encapsulated cells within the hydrogel systems. The cells encapsulated into the gels included hematopoietic stem cells as well as OP9-DL1 stromal cells. The incorporation of gelatin in the hydrogels resulted in visual attachment and elongation of the OP9-DL1 cells not seen in the hydrogels without gelatin. **Figure 3.1** shows light microscope images (10X magnification) of the gels encapsulating 5,000 ckit+sca1+ cells and 20,000 OP9-DL1 in 250 μL hydrogel cocultures on day 3. This behavior of the OP9-DL1 may influence the ligand presentation and interaction between the cells and thereby influence the differentiation of the HSCs.

Rheology studies were performed to compare the mechanical properties of the hydrogels with that of the thymus. The storage modulus was measured using a rheometer to obtain data on the viscoelastic properties of the gels. The storage modulus was measured for various hydrogels and mouse thymus tissue samples as representative value of the elastic portion of the material's resistance to deformation. The samples were placed on the rheometer between cylindrical plates and deformed by oscillatory strain applied by

the rotation of the plates. To choose proper frequency and strains for testing, frequency and strain sweep measurements were initially performed on the gels and the appropriate values were determined based on linear regions in the sweeps (**Figure 3.2**). Based on the linear regions of the sweeps, measurements were taken at 1 Hz and 5% strain, same as values reported for the mouse thymus.

Hydrogels of total 250 μL were prepared in silicone molds and varied in different crosslinking densities. The crosslinking densities were varied but adjusting the w/v concentration of PEG component added to the gels. Gels were synthesized with PEG at a concentration of 1%, 2%, or 4% (w/v). However, the hydrogels with 1% (w/v) PEG were too soft to get an accurate reading from the rheometer due to too much slippage. All gels were composed of 1% (w/v) HA and, if gelatin was included, it was also at a concentration of 1% (w/v). **Figure 3.3** shows the storage modulus values for the various hydrogels as well as the thymus, taken from 4 to 8 week old female BALB/c mice. Each measurement represents at least n=4 samples. As shown, the gelatin component had a significant impact on the hydrogel mechanical properties and in both PEGDA and PEGSSDA gels, the addition of gelatin greatly decreased the storage modulus. The storage modulus for gels with gelatin at a concentration of 1% (w/v) was determined to be approximately 49.20 Pa, 99.63 Pa, 19.23 Pa, and 34.47 Pa for gels with PEGDA (2%), PEGDA (4%), PEGSSDA (2%), and PEGSSDA (4%) respectively. The gels without a gelatin component had storage modulus determined to be approximately 113.25 Pa, 149.75 Pa, 73.52 Pa, and 89.32 Pa for gels composed of PEGDA (2%), PEGDA (4%), PEGSSDA (2%), and PEGSSDA (4%) respectively. The gels composed of PEGSSDA (**Figure 3.3A**) also had lower storage modulus values when compared to PEGDA gels (**Figure 3.3B**) with same concentration. These gels allowed us to mimic the thymic microenvironment in terms of matric elasticity more closely and compare the

differentiation of T cells in terms of hydrogel environment. The thymus storage modulus was in agreement with studies comparing rheological measurements of bulk central nervous system tissue with scanning electron microscope measurements of individual cells [16].

The hydrogels were modified with DLL4 through biotinylated ligand attachment via acrylated PEG-Streptavidin. The PEG component of the hydrogel was first modified with streptavidin than added in ratio with biotinylated DLL4 into the hydrogels. To quantify the ligand density within the gels FITC labeled biotin-BSA, biotin-BSA-FITC, was used as a substitute to mimic ligand incorporation. Three different ligand densities were tested. The ligand was measured out in ratio to the PEG component added, 1:500, 1:1000, 1:5000. The 1:500 ratio of ligand to PEG did not result in a solid gel, caused by too much ligand present interfering with the crosslinking of PEG. The two remaining ratios were measured for fluorescence to interpret potential ligand density. For each ratio, three gels (n=3) were prepared and the data was pooled together to get a strong enough fluorescent reading. The gels were thoroughly washed before fluorescent measurements were taken to accurately determine the amount of biotin-BSA-FITC immobilized within the gels. Streptavidin density was kept constant and density of biotin-BSA-FITC at within gels composed of 1% HA and 2% or 4% PEG are shown in **Figure 3.4**. **Figure 3.4A** shows 1:1000 ligand to PEG ratio while **Figure 3.4B** shows the incorporation after addition of 1:5000 ligand to PEG ratio. In both, more ligand is incorporated within the 2% PEG gels than the 4% PEG gels. In **Figure 3.4A** 1.8890 pmol/mL gel is measured in the 4% gel versus 1.8896 pmol/mL gel in the 2% gel. In **Figure 3.4B** 0.3621 pmol/mL is measured in the 4% gel and 0.3622 pmol/mL is measured in the 2% gel. This indicates that with lower crosslinking, there is higher incorporation of the ligand.

3.3.2 Differentiation Results

3.3.2.1 HSC and OP9-DL1 2D and 3D Cocultures

The differentiation of 2D coculture was compared to 3D hydrogel coculture encapsulating Lin-ckit+sca1+ cells with OP9-DL1 cells. The Zúñiga-Pflücker group has developed a protocol for the expansion and differentiation of murine bone marrow HSCs on OP9-DL1 cultures in tissue culture dishes adopted here to compare with 3D encapsulation differentiation. Three different gels were tested of varying composition. Gel A, in this study, represents HA (1%) - PEGSSDA (2%), Gel B represents HA (1%)- PEGSSDA (4%), and Gel C represents HA (1%)- Gelatin (1%)- PEGSSDA (2%) hydrogel.

On day 8, the cells population was removed from the 2D cocultures by pipetting and gently removing the cells then straining through a 40 μm cell strainer to remove the OP9-DL1 cells. The hydrogels were degraded by dissolution process using 50mM N-acetyl-L-cysteine solution and mixing over 30 minutes before complete dissolution of gel. The suspension was then also passed through a 40 μm cell strainer to remove the stromal cells. The cells were then analyzed for cell markers Thy 1.2, CD19, CD25, and CD44 (**Figure 3.5**). Thy1.2 is a pan-T cell marker and has been used to report early T lineage generation. CD19 is a B cell marker and would be expected to be expressed if the HSCs were cocultured in the presence of OP9 cells lacking Notch ligand. All samples show low levels of CD19 expression. However, we report the generation of Thy1.2+ cells at higher percentages in the 2D coculture than any of the 3D hydrogel cocultures. The cells were analyzed for CD25 and CD44 markers to determine which stage of development T cells were in. As described earlier, the primary steps during T cell development include the double negative (DN) stages where the cells transition sequentially through DN1 (CD44+CD25), DN2 (CD44+CD25+), DN3 (CD44-CD25+),

and DN4 (CD44-CD25-) stages while traveling from the cortico-medullary junction through the outer cortex to the subcapsular zone of the thymus. The results show that in all samples, the majority of early T cells expressing Thy1.2 were in the DN1 and DN2 stages of development. This correlates with previous findings of 2D cocultures.

3.3.2.2 Differentiation of bone marrow HSCs using DLL4 immobilized surfaces and hydrogels

Although the coculture of stems cells seeded onto OP9-DL1 cells (bone marrow stromal cells transfected to present immobilized Notch ligand DLL1) have been successful in *in vitro* T cell differentiation [12], [24], [50]–[52], approaches without the use of OP9-DL1 cells are still highly desirable. Stroma-free approaches off the advantage of avoiding the contamination of animal stromal cells, such as the OP9-DL1 cell line created from bone marrow stromal cells transfected to present immobilized Notch ligand DLL1. One such method that has been successful is DLL4 immobilized on the surface of microbeads supporting early T-lineage specification of HPCs [49]. Three different methods, each utilizing 5,000 Lin-ckit+sca1+ cells were tested in this report that may use stromal cells but not in contact with HPCs.

The first was a previously studied method of ligand coated 2D culture surface using and defined media with a cocktail of cytokines (IL-6, Flt-3L, SCF, IL-7 and IL-11, as defined by Varnum-Finney, et al.). DLL4 (R&D Systems) was biotinylated by using the Biotin-XX Microscale Protein Labeling Kit (Invitrogen) then coated on plates modified with streptavidin. The bone marrow HSCs, Lin-ckit+sca1+ cells, were then seeded on top of the bDLL4 coated surface. The second design was the same system except that a cell culture insert with confluent OP9-DL1 cells was added with OP9-DL1 media (stated in methods) and only IL-7 and Flt-3L cytokine cocktail. Thirdly, bDLL4 was incorporated into HA (1%) – PEGDA (2%) gels via acrylated PEG-Streptavidin. The

PEG component of the hydrogel was first modified with streptavidin than added in ratio (1:1000 and 1:5000) with biotinylated DLL4 into the hydrogels. The gels, encapsulating bone marrow HSCs, were formed within cell culture inserts in well plates with a confluent layer of OP9-DL1 cells plated and exposed to OP9-DL1 media with IL-7 and Flt-3L cytokine cocktail.

Day 8 analysis was performed on the bone marrow HSCs. Each condition had n=3 samples. On day 8, cells were isolated and strained in a 40 μm cell strainer before being pooled together for each condition and analyzed on flow cytometer. 7-AAD staining allowed the dead cells to be excluded from the analysis. Cells were stained with anti-CD25 and anti-CD44 antibodies. The results, as shown in **Figure 3.6**, indicated that cells began differentiation into the DN1 stage of development, characterized by CD44+CD25-, the population in the upper left quadrant. The plated system with defined media and no OP9-DL1 was the only system to also show a population of cells in DN2 stage, CD44+CD25+. **Figure 3.7A** shows the percent of Thy1.2 positive cells in each condition. The results show great increase in Thy1.2 expressing cells, indicating early T cells, in plates with 2 mg of bDLL4 and defined media, 6.056% Thy1.2+ cells versus 0.671% in plates with no bDLL4. In plates with bDLL4 and OP9-DL1 inserts, the percentage of Thy1.2+ cells did not change significantly, both the plate with 2 mg of bDLL4 and the plate with no bDLL4 showed approximately 2.5% Thy1.2+ cells. For the hydrogel system incorporating bDLL4 and HSCs, the percentages of cells expressing the Thy1.2 marker were high, 5.888% and 6.06%, in the gels with 1:1000 and 1:5000 PEG to bDLL4 ratio respectively. **Figure 3.7B** shows which DN stage the Thy1.2+ cells belong according to their expression of CD25 and CD44. However, due to lack of precise gating the cells within DN4 stage, CD44-CD25-, may represent cells not differentiated at all.

3.3.2.3 Encapsulation of R1 ES and iPS cells using DLL-presenting cells or beads in hydrogels

In addition to Lin-ckit+sca1+ cells, murine embryonic stem cells (R1, Nagy Lab) and murine induced pluripotent stem (iPS) cells (iPS- MEF-Ng-20D-17, Riken Cell Bank) were studied. The differentiation of 2D OP9-DL1 coculture was compared to 3D hydrogel encapsulation of R1 or iPS cells with OP9-DL1 cells in a coculature of bDLL4 beads. R1 and iPS cells were expanded on MEF feeder layers. 1 x 10^5 R1 or iPS cells were plated onto OP9-DL1 monolayers (80% confluent) for a 2D coculture. The hydrogel 3D cocultures consisted of encapsulating 1 x 10^5 R1 or iPS cells with either 1 x 10^5 OP9-DL1 cells or 1 x 10^6 beads coated with bDLL4 (resulting in a 10 to 1 bead to R1/iPS cell ratio). Hydrogels components were purchased from Glycosan and composed of thiol-modified HA (1%), thiol-modified gelatin (1%), and the thiol-reactive crosslinker, PEG (2%) (w/v). The gel components were added in a total of 250 μL of degassed water containing the cells and/or beads. After a gelation period of 30 minutes, 250 μL of media was added containing a cytokine cocktail of IL-7 and Flt-3L, as defined by Zúñiga-Pflücker, et al. The 2D plated cocultures were passaged and maintained as defined by the previously established protocol by Zúñiga-Pflücker. The hydrogel cocultures had media changes every 3-4 days but were not passaged until day 12 and day 20 when the gels were degraded by 10% hyaluronidase and the cells analyzed.

Cells were analyzed by flow cytometry for CD25, CD44, CD4, and CD8 on days 12 and 20. The R1 cells differentiation data (**Figure 3.8**) shows distinct population of CD25+CD44- cells, indicative of early T cells in the double negative 1 (DN1) stage. The differentiation data for Day 20 shows large DN1 and DN2 stage cells for the plated cocultures. However, there is little change in the cells in the gel conditions showing no

progression in T cell differentiation. Additionally, no significant CD4+ or CD8+ cell populations were noticed in any conditions at either time point (data not shown).

The differentiation data for the iPS cells (**Figure 3.9**) similarly showed distinct populations of DN1 stage cells at Day 12 for all conditions. However, the transition from day 12 to day 20 revealed a decrease in that population and no further distinct populations. Also, as seen in the R1 cells, there was no CD4+ or CD8+ cell populations in any conditions at either time point (data not shown).

Figure 3.1 Light microscopy images of encapsulated cells in hydrogels

Representative hydrogels were imaged (10X magnification) on day 3 of 5,000 ckit+sca1+ cells and 20,000 OP9-DL1 in 250 μL hydrogel cocultures. A 2D plated control was imaged showing 5,000 ckit+sca1+ cells seeded onto an 80% confluent layer of O9-DL1 cells. Hydrogels that are imaged are HA (1%) – PEG (2%) (B), HA (1%) – PEG (4%) (C), and HA (1%) – PEG (2%) – Gelatin (1%) (D).

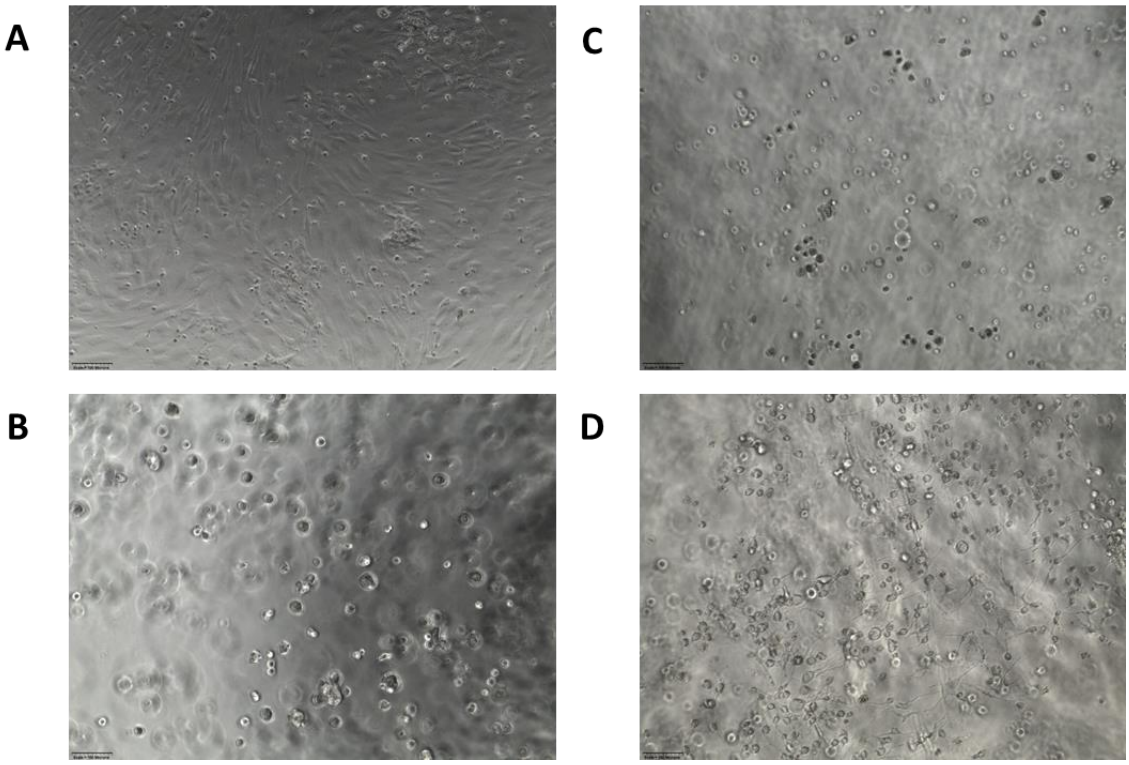

Figure 3.2 Rheology studies: Frequency sweep and strain sweep

Frequency sweeps (A) and strain sweeps (B) were performed on the gels at room temperature in order to determine a good frequency and strain to measure the storage modulus of the materials. Measurements were taken at 1 Hz frequency and 5% strain, as these conditions were in the linear regions of representative frequency and amplitude sweeps for all hydrogel types and mouse thymus.

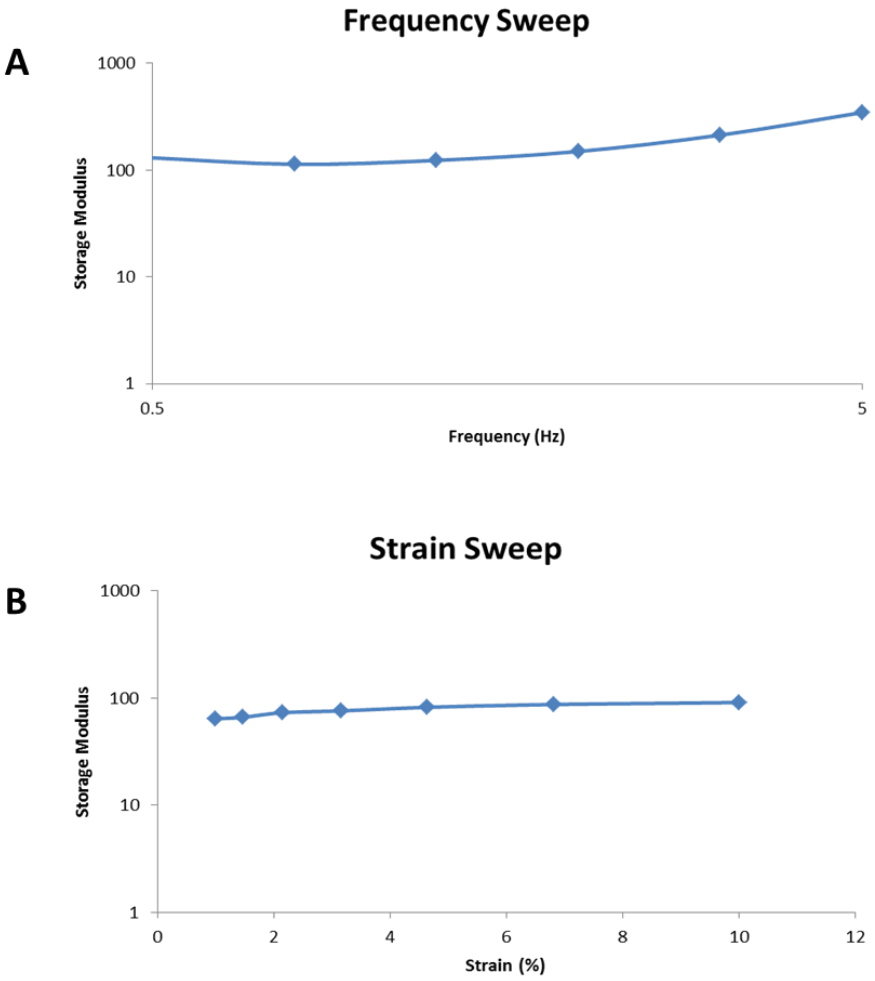

Figure 3.3 Rheology studies: Storage modulus measurements of hydrogels and mouse thymus

The storage modulus was measured for various hydrogels and mouse thymus tissue samples as representative value of the elastic portion of the material's resistance to deformation. The samples were placed on the rheometer between cylindrical plates and deformed by oscillatory strain applied by the rotation of the plates. The storage modulus was measured at 1 Hz frequency and 5% strain. Hydrogels tested included those composed of PEGDA (A) and PEGSSDA (B).

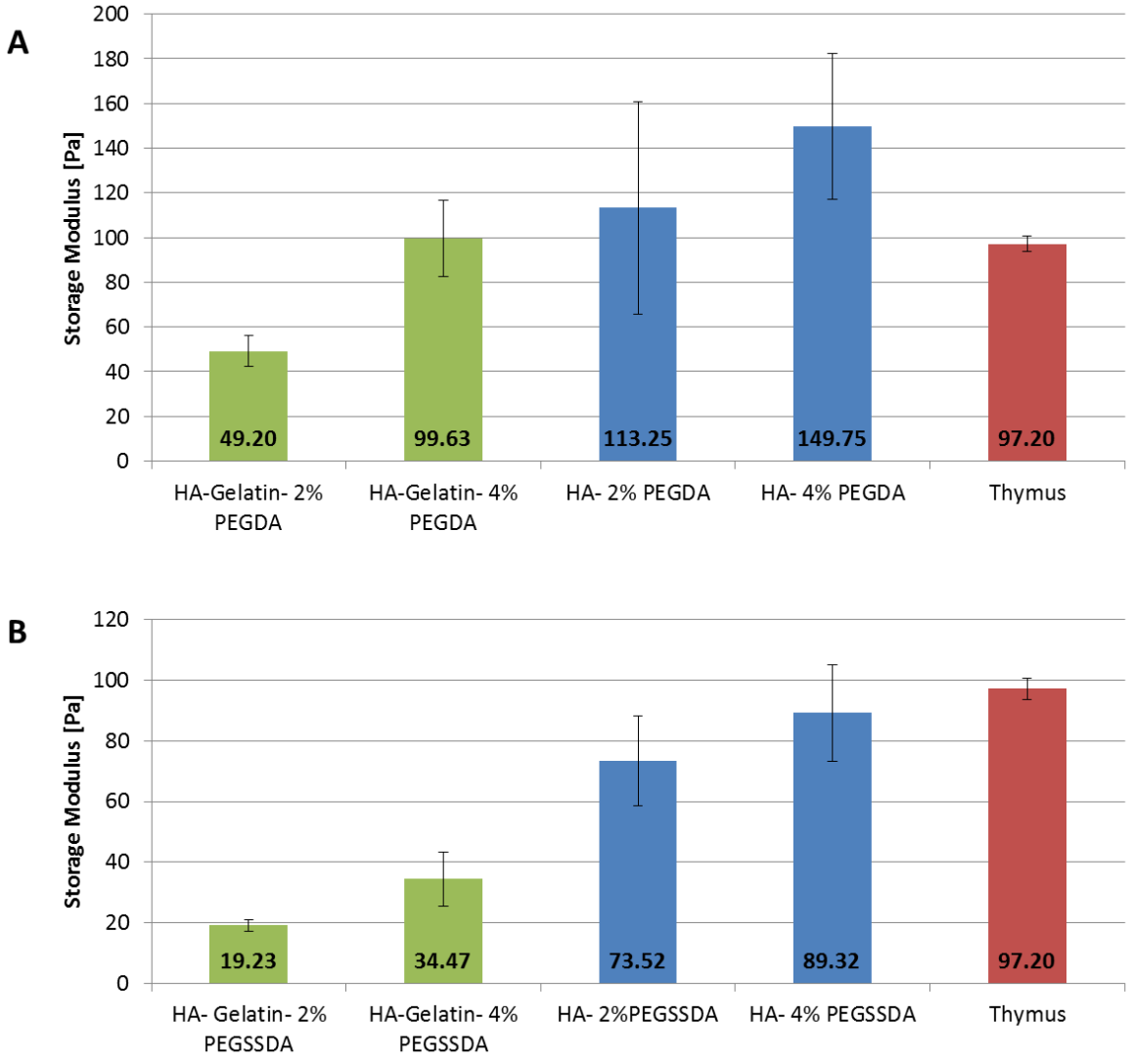

Figure 3.4 Molar density of biotin-FITC incorporated into gels via acrylated PEG streptavidin

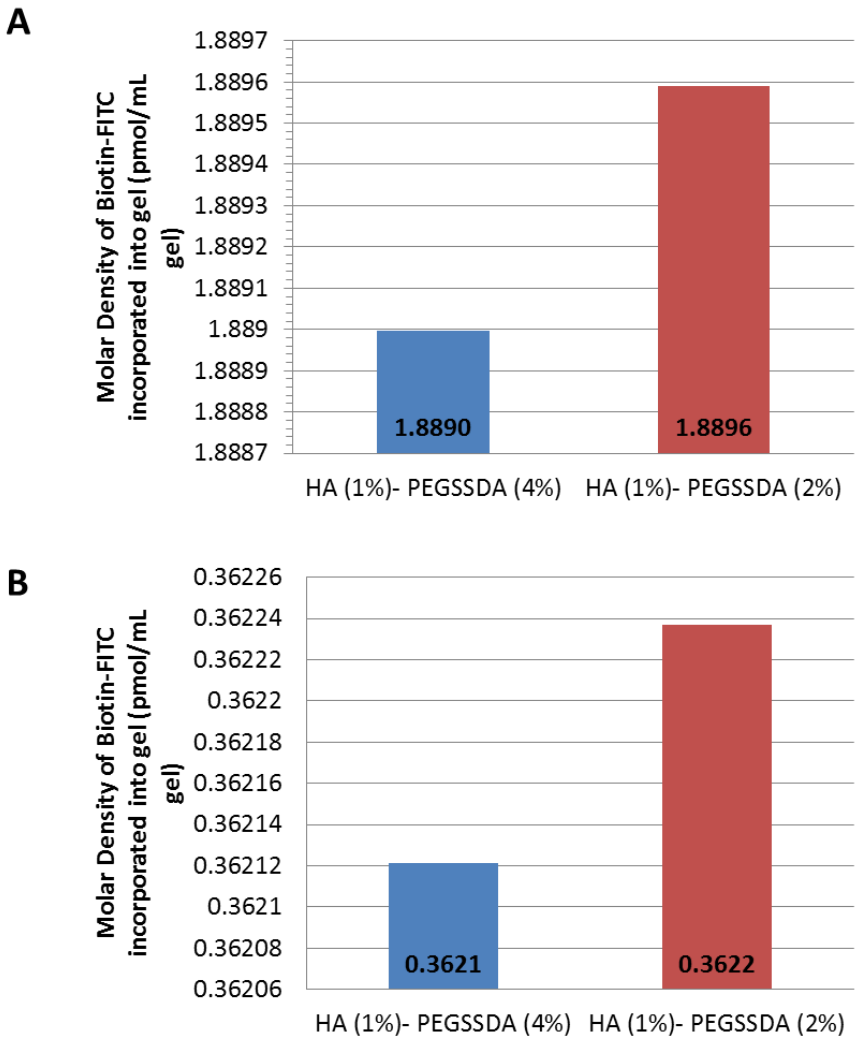

Figure 3.5 Murine bone marrow hematopoietic stem cells and OP9-DL1 cocultures encapsulated in hydrogels

Murine bone marrow hematopoietic stem cells, Lin-ckit+sca1+, were cocultured with OP9-DL1 cells on a plate or encapsulated with OP9-DL1 cells in hydrogels in the presence of cytokine cocktails. Differentiation data is shown from flow cytometry analysis on day 8 for Thy1.2, CD19, CD25, and CD44 markers

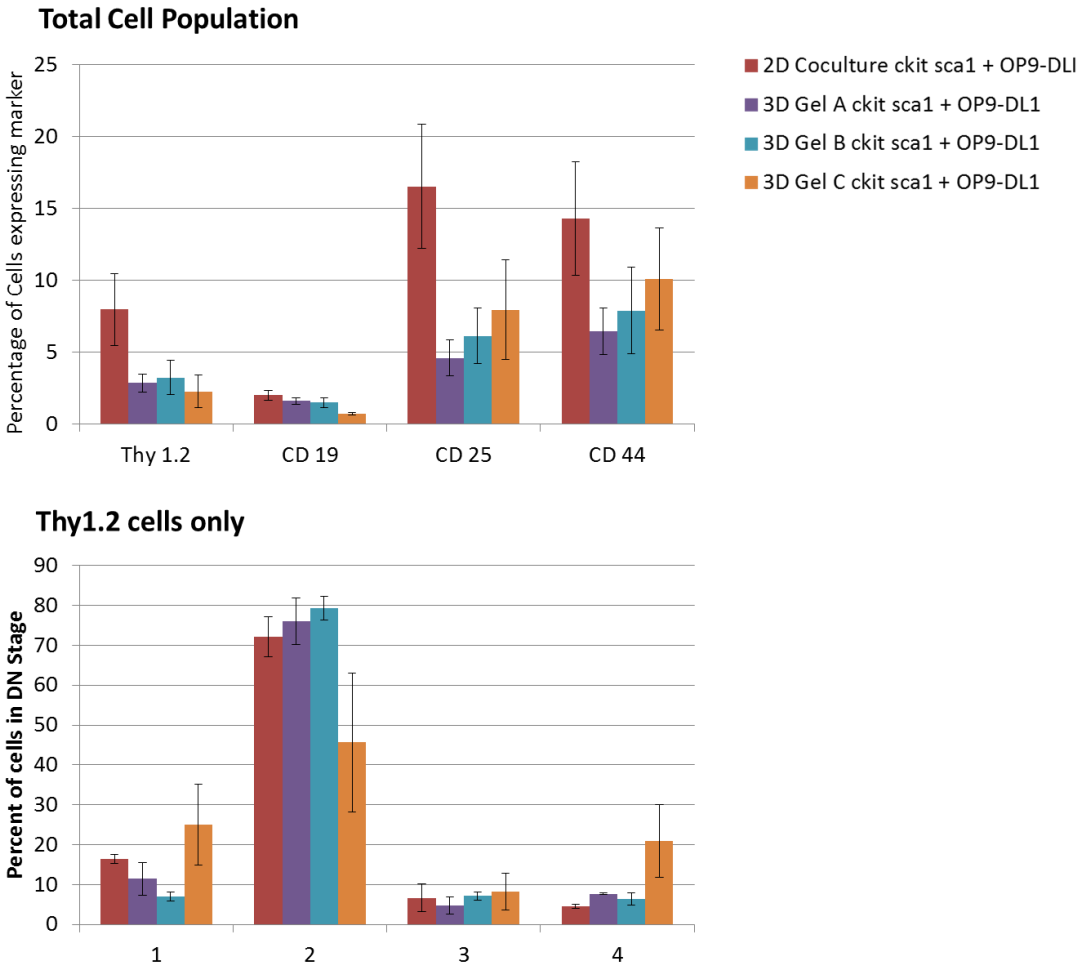

Figure 3.6 Differentiation results of DLL4 approaches

Murine bone marrow hematopoietic stem cells, Lin-ckit+sca1+, were plated or encapsulated in hydrogels in the presence of immobilized DLL4. Differentiation data is shown from flow cytometry analysis on day 8 for CD25, and CD44 markers.

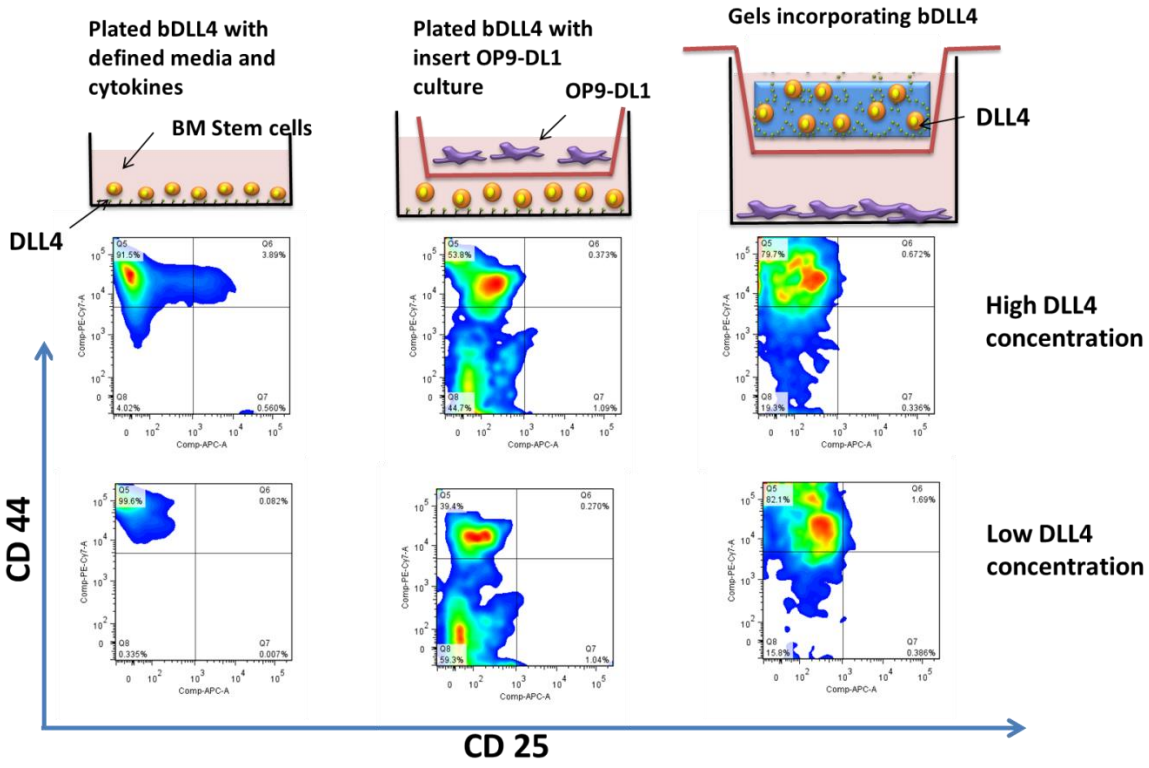

Figure 3.7 Differentiation results of immobilized DLL4 approaches: Thy1.2 positive cells and their DN stages

Murine bone marrow hematopoietic stem cells, Lin-ckit+sca1+, were plated or encapsulated in hydrogels in the presence of immobilized DLL4. Differentiation data is shown from flow cytometry analysis on day 8 for expression of Thy1.2 (A) and CD25 and CD44 markers (B).

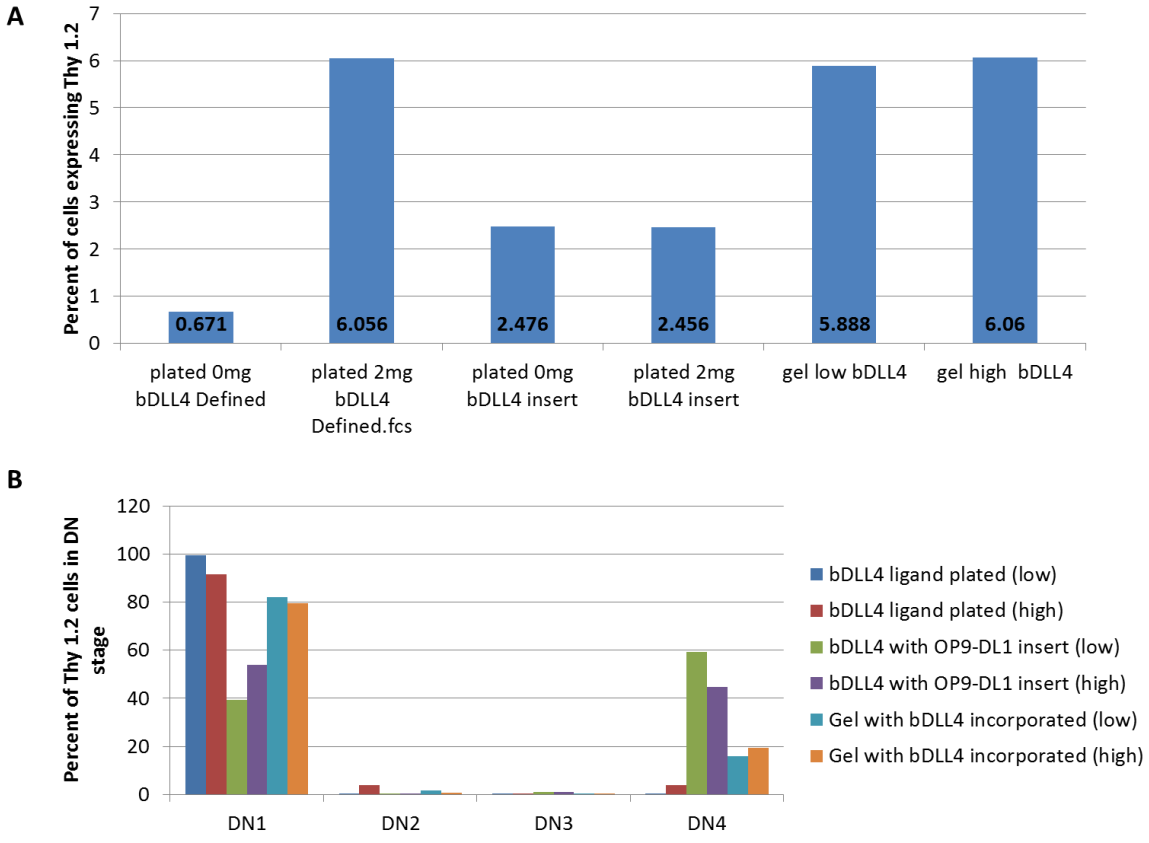

Figure 3.8 Murine embryonic (R1) stem cells differentiation results

Murine embryonic stem cells (R1) were cocultured with OP9-DL1 cells on a plate or encapsulated with OP9-DL1 cells or bDLL4 beads in HA-Gelatin-PEGDA gels in the presence of cytokine cocktails. Differentiation data is shown from flow cytometry analysis on day 12 and day 20 for CD25 and CD44 markers.

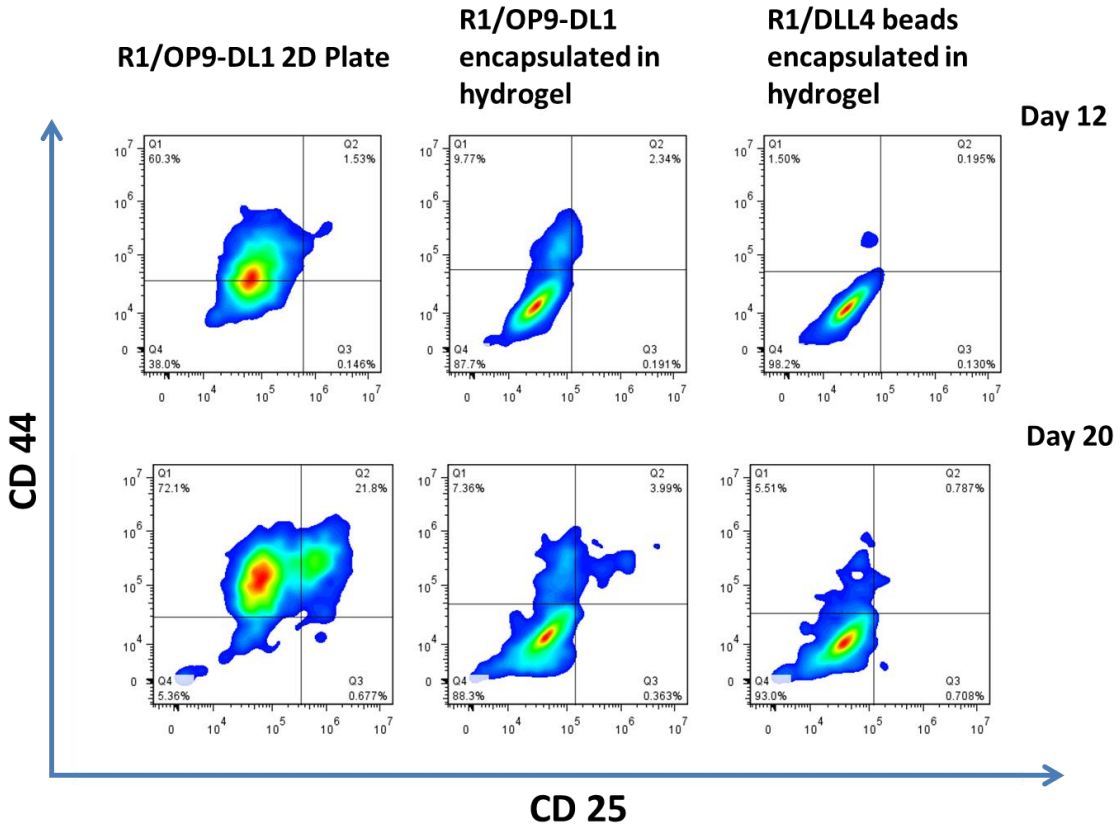

Figure 3.9 Murine induced pluripotent stem (iPS) cells differentiation results

Murine induced pluripotent stem cells (iPS) were cocultured with OP9-DL1 cells on a plate or encapsulated with OP9-DL1 cells or bDLL4beads in HA-Gelatin-PEGDA gels in the presence of cytokine cocktails. Differentiation data is shown from flow cytometry analysis on day 12 and day 20 for CD25 and CD44 markers.

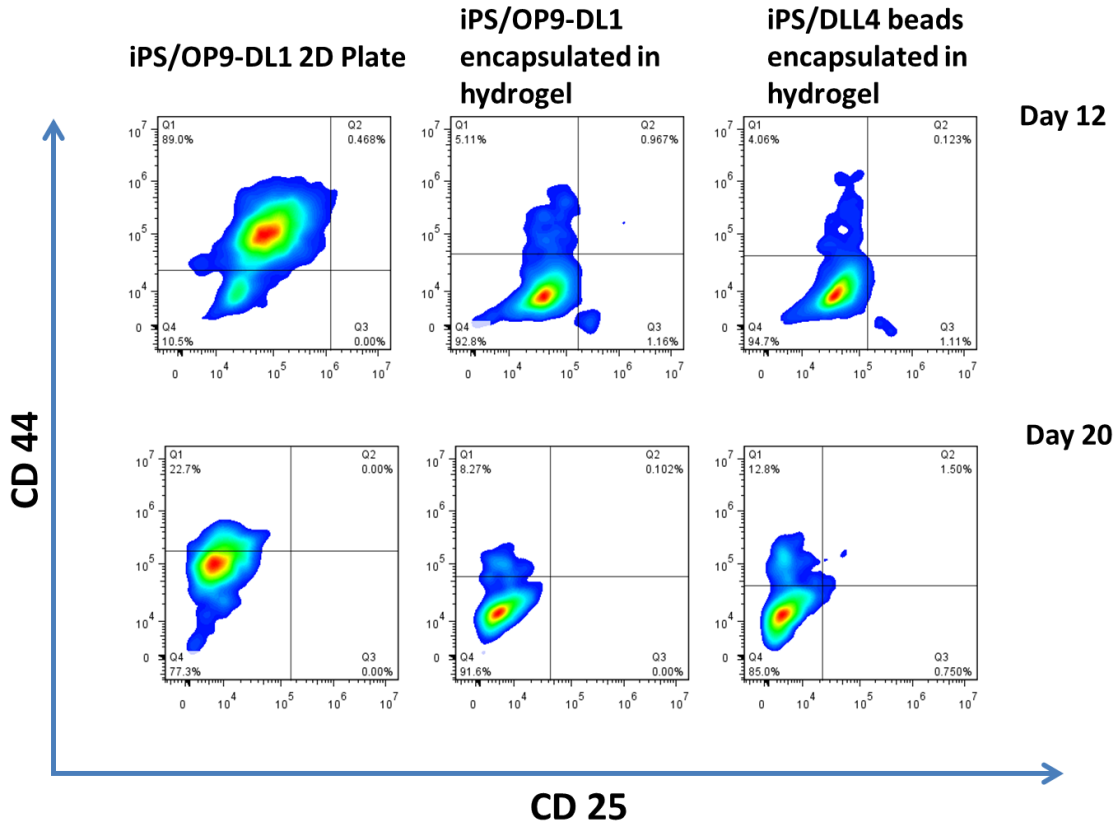

3.4 REFERENCES

[1] J. S. Miller, "Successful adoptive transfer and in vivo expansion of human haploidentical NK cells in patients with cancer," *Blood*, vol. 105, no. 8, pp. 3051–7, Apr. 2005.

[2] G. E. Plautz, R. M. Bukowski, A. C. Novick, E. A. Klein, E. D. Kursh, T. E. Olencki, R. J. Yetman, A. Pienkny, K. Sandstrom, and S. Shu, "T-cell adoptive immunotherapy of metastatic renal cell carcinoma," *Urology*, vol. 54, no. 4, pp. 617–623, Oct. 1999.

[3] C. Yee, "Adoptive T-Cell Therapy of Cancer," *Immunother. Cancer*, vol. 20, no. 3, pp. 711–733, Jun. 2006.

[4] S. A. Rosenberg and M. E. Dudley, "Adoptive cell therapy for the treatment of patients with metastatic melanoma," *Lymph. Dev. Tumour Immunol. Ed. Casey Weav. Alexander Rudensky Ton Schumacher Nick Restifo*, vol. 21, no. 2, pp. 233–240, Apr. 2009.

[5] M. E. Dudley and S. A. Rosenberg, "Adoptive-cell-transfer therapy for the treatment of patients with cancer," *Nat Rev Cancer*, vol. 3, no. 9, pp. 666–675, Sep. 2003.

[6] G. Q. Daley, "Realistic prospects for stem cell therapeutics," *Hematology*, pp. 398–418, 2003.

[7] G. Q. DALEY, "From Embryos to Embryoid Bodies," *Ann. N. Y. Acad. Sci.*, vol. 996, no. 1, pp. 122–131, May 2003.

[8] J. C. Zuniga-Pflucker, "T-cell development made simple," *Nat Rev Immunol*, vol. 4, no. 1, pp. 67–72, Jan. 2004.

[9] K. Laky, C. Fleischacker, and B. J. Fowlkes, “TCR and Notch signaling in CD4 and CD8 T-cell development.,” *Immunol. Rev.*, vol. 209, no. 1, pp. 274–283, Feb. 2006.

[10] R. N. Germain, “T-cell development and the CD4-CD8 lineage decision,” *Nat Rev Immunol*, vol. 2, no. 5, pp. 309–322, May 2002.

[11] M. Ciofani and J. C. Zúñiga-Pflücker, “The Thymus as an Inductive Site for T Lymphopoiesis,” *Annu. Rev. Cell Dev. Biol.*, vol. 23, no. 1, pp. 463–493, Oct. 2007.

[12] T. M. Schmitt and J. C. Zúñiga-Pflücker, “Induction of T Cell Development from Hematopoietic Progenitor Cells by Delta-like-1 In Vitro,” *Immunity*, vol. 17, no. 6, pp. 749–756, Dec. 2002.

[13] B. L. Beckstead, D. M. Santosa, and C. M. Giachelli, “Mimicking cell–cell interactions at the biomaterial–cell interface for control of stem cell differentiation,” *J. Biomed. Mater. Res. A*, vol. 79A, no. 1, pp. 94–103, Oct. 2006.

[14] D. J. Izon, J. A. Punt, and W. S. Pear, “Deciphering the role of Notch signaling in lymphopoiesis,” *Curr. Opin. Immunol.*, vol. 14, no. 2, pp. 192–199, Apr. 2002.

[15] S. M. Lehar and M. J. Bevan, “T Cell Development in Culture,” *Immunity*, vol. 17, no. 6, pp. 689–692, Dec. 2002.

[16] M. E. Carlson, “Notch signaling pathway and tissue engineering,” *Front. Biosci.*, vol. 12, pp. 5143–56, 2007.

[17] U. Koch, E. Fiorini, R. Benedito, V. Besseyrias, K. Schuster-Gossler, M. Pierres, N. R. Manley, A. Duarte, H. R. MacDonald, and F. Radtke, “Delta-like 4 is the essential, nonredundant ligand for Notch1 during thymic T cell lineage commitment,” *J. Exp. Med.*, vol. 205, no. 11, pp. 2515–2523, Oct. 2008.

[18] D. M. Gravano and J. O. Manilay, “Inhibition of proteolysis of Delta-like-1 does not promote or reduce T-cell developmental potential.,” *Immunol. Cell Biol.*, vol. 88, no. 7, pp. 746–753, Oct. 2010.

[19] K. Hozumi, C. Mailhos, N. Negishi, K. Hirano, T. Yahata, K. Ando, S. Zuklys, G. A. Holländer, D. T. Shima, and S. Habu, “Delta-like 4 is indispensable in thymic environment specific for T cell development,” *J. Exp. Med.*, vol. 205, no. 11, pp. 2507–2513, Oct. 2008.

[20] M. Mohtashami, D. K. Shah, H. Nakase, K. Kianizad, H. T. Petrie, and J. C. Zúñiga-Pflücker, “Direct Comparison of Dll1- and Dll4-Mediated Notch Activation Levels Shows Differential Lymphomyeloid Lineage Commitment Outcomes,” *J. Immunol.*, vol. 185, no. 2, pp. 867–876, Jul. 2010.

[21] M. H. Dallas, B. Varnum-Finney, C. Delaney, K. Kato, and I. D. Bernstein, “Density of the Notch ligand Delta1 determines generation of B and T cell precursors from hematopoietic stem cells,” *J. Exp. Med.*, vol. 201, no. 9, pp. 1361–1366, May 2005.

[22] S. K. Cho, T. D. Webber, J. R. Carlyle, T. Nakano, S. M. Lewis, and J. C. Zúñiga-Pflücker, “Functional Characterization of B Lymphocytes Generated in vitro from Embryonic Stem Cells,” *Proc. Natl. Acad. Sci. U. S. A.*, vol. 96, no. 17, pp. 9797–9802, Aug. 1999.

[23] T. Nakano, H. Kodama, and T. Honjo, “Generation of Lymphohematopoietic Cells from Embryonic Stem Cells in Culture,” *Science*, vol. 265, no. 5175, pp. 1098–1101, Aug. 1994.

[24] E. J. Jenkinson and G. Anderson, “Fetal thymic organ cultures,” *Curr. Opin. Immunol.*, vol. 6, no. 2, pp. 293–297, Apr. 1994.

[25] T. M. Schmitt and J. C. Zúñiga-Pflücker, “T-cell development, doing it in a dish.,” *Immunol. Rev.*, vol. 209, no. 1, pp. 95–102, Feb. 2006.

[26] F. Radtke, A. Wilson, G. Stark, M. Bauer, J. van Meerwijk, H. R. MacDonald, and M. Aguet, “Deficient T Cell Fate Specification in Mice with an Induced Inactivation of Notch1,” *Immunity*, vol. 10, no. 5, pp. 547–558, May 1999.

[27] J. C. Pui, D. Allman, L. Xu, S. DeRocco, F. G. Karnell, S. Bakkour, J. Y. Lee, T. Kadesch, R. R. Hardy, J. C. Aster, and W. S. Pear, “Notch1 Expression in Early Lymphopoiesis Influences B versus T Lineage Determination,” *Immunity*, vol. 11, no. 3, pp. 299–308, Sep. 1999.

[28] B. Varnum-Finney, “Immobilization of Notch ligand, Delta-1, is required for induction of notch signaling,” *J. Cell Sci.*, vol. 113 Pt 23, pp. 4313–8, 2000.

[29] B. Varnum-Finney, “Combined effects of Notch signaling and cytokines induce a multiple log increase in precursors with lymphoid and myeloid reconstituting ability,” *Blood*, vol. 101, no. 5, pp. 1784–9, Mar. 2003.

[30] J. Lee and N. A. Kotov, “Notch Ligand Presenting Acellular 3D Microenvironments for ex vivo Human Hematopoietic Stem-Cell Culture made by Layer-By-Layer Assembly,” *Small*, vol. 5, no. 9, pp. 1008–1013, May 2009.

[31] G. Anderson and Y. Takahama, “Thymic epithelial cells: working class heroes for T cell development and repertoire selection,” *Spec. Focus Struct. Funct. Lymphoid Tissues*, vol. 33, no. 6, pp. 256–263, Jun. 2012.

[32] S. Berrih, “Extracellular matrix of the human thymus: immunofluorescence studies on frozen sections and cultured epithelial cells,” *J. Histochem. Cytochem.*, vol. 33, no. 7, pp. 655–64, 1985.

[33] M. P. Lutolf, P. M. Gilbert, and H. M. Blau, “Designing materials to direct stem-cell fate,” *Nature*, vol. 462, no. 7272, pp. 433–441, Nov. 2009.

[34] A. J. Engler, S. Sen, H. L. Sweeney, and D. E. Discher, “Matrix Elasticity Directs Stem Cell Lineage Specification,” *Cell*, vol. 126, no. 4, pp. 677–689, Aug. 2006.

[35] C. Cha, W. B. Liechty, A. Khademhosseini, and N. A. Peppas, “Designing Biomaterials To Direct Stem Cell Fate,” *ACS Nano*, vol. 6, no. 11, pp. 9353–9358, Nov. 2012.

[36] K. Ghosh, Z. Pan, E. Guan, S. Ge, Y. Liu, T. Nakamura, X.-D. Ren, M. Rafailovich, and R. A. F. Clark, “Cell adaptation to a physiologically relevant ECM mimic with different viscoelastic properties,” *Biomaterials*, vol. 28, no. 4, pp. 671–679, Feb. 2007.

[37] J. Holst, S. Watson, M. S. Lord, S. S. Eamegdool, D. V. Bax, L. B. Nivison-Smith, A. Kondyurin, L. Ma, A. F. Oberhauser, A. S. Weiss, and J. E. J. Rasko, “Substrate elasticity provides mechanical signals for the expansion of hemopoietic stem and progenitor cells,” *Nat Biotech*, vol. 28, no. 10, pp. 1123–1128, Oct. 2010.

[38] R. S. O’Connor, “Substrate rigidity regulates human T cell activation and proliferation,” *J. Immunol. 1950*, vol. 189, no. 3, pp. 1330–9, Aug. 2012.

[39] M. P. Lutolf, R. Doyonnas, K. Havenstrite, K. Koleckar, and H. M. Blau, "Perturbation of single hematopoietic stem cell fates in artificial niches," *Integr. Biol.*, vol. 1, no. 1, pp. 59–69, 2009.

[40] K. Y. Lee and D. J. Mooney, "Hydrogels for Tissue Engineering," *Chem. Rev.*, vol. 101, no. 7, pp. 1869–1880, May 2001.

[41] D. N. Haylock and S. K. Nilsson, "The role of hyaluronic acid in hemopoietic stem cell biology," *Regenerative Medicine*, vol. 1, no. 4, p. 437+, Jul-2006.

[42] M. I. Tammi, "Hyaluronan and homeostasis: a balancing act," *J. Biol. Chem.*, vol. 277, no. 7, pp. 4581–4, Feb. 2002.

[43] J. R. E. Fraser, T. C. Laurent, and U. B. G. Laurent, "Hyaluronan: its nature, distribution, functions and turnover," *J. Intern. Med.*, vol. 242, no. 1, pp. 27–33, Jul. 1997.

[44] Sharon Gerecht, Jason A. Burdick, L. S. Ferreira, S. A. Townsend, R. Langer, and G. Vunjak-Novakovic, "Hyaluronic Acid Hydrogel for Controlled Self-Renewal and Differentiation of Human Embryonic Stem Cells," *Proc. Natl. Acad. Sci. U. S. A.*, vol. 104, no. 27, pp. 11298–11303, Jul. 2007.

[45] G. D. Prestwich, "Hyaluronic acid-based clinical biomaterials derived for cell and molecule delivery in regenerative medicine," *Proc. Fifthteenth Int. Symp. Recent Adv. Drug Deliv. Syst.*, vol. 155, no. 2, pp. 193–199, Oct. 2011.

[46] X. Z. Shu, Y. Liu, F. Palumbo, and G. D. Prestwich, "Disulfide-crosslinked hyaluronan-gelatin hydrogel films: a covalent mimic of the extracellular matrix for in vitro cell growth," *Biomaterials*, vol. 24, no. 21, pp. 3825–3834, Sep. 2003.

[47] X. Zheng Shu, Y. Liu, F. S. Palumbo, Y. Luo, and G. D. Prestwich, “In situ crosslinkable hyaluronan hydrogels for tissue engineering,” *Biomaterials*, vol. 25, no. 7–8, pp. 1339–1348, Mar. 2004.

[48] J. Zhang, A. Skardal, and G. D. Prestwich, “Engineered extracellular matrices with cleavable crosslinkers for cell expansion and easy cell recovery,” *Biomaterials*, vol. 29, no. 34, pp. 4521–4531, Dec. 2008.

[49] S. Taqvi, L. Dixit, and K. Roy, “Biomaterial-based notch signaling for the differentiation of hematopoietic stem cells into T cells,” *J. Biomed. Mater. Res. A*, vol. 79A, no. 3, pp. 689–697, Dec. 2006.

[50] T. M. Schmitt, R. F. de Pooter, M. A. Gronski, S. K. Cho, P. S. Ohashi, and J. C. Zuniga-Pflucker, “Induction of T cell development and establishment of T cell competence from embryonic stem cells differentiated in vitro,” *Nat Immunol*, vol. 5, no. 4, pp. 410–417, Apr. 2004.

[51] R. N. La Motte-Mohs, “Induction of T-cell development from human cord blood hematopoietic stem cells by Delta-like 1 in vitro,” *Blood*, vol. 105, no. 4, pp. 1431–9, Feb. 2005.

[52] M. De Smedt, I. Hoebeke, and J. Plum, “Human bone marrow CD34+ progenitor cells mature to T cells on OP9-DL1 stromal cell line without thymus microenvironment,” *Work. Haploidentical Hematop. Stem Cell Transplant.*, vol. 33, no. 3, pp. 227–232, Nov. 2004.

Chapter 4: Conclusions

The objective of this thesis work was to utilize the advantages of PEG based hydrogel systems for disease-specific pulmonary drug delivery of therapeutic agents and *in vitro* T cell differentiation of mouse bone marrow HSC, ES, and iPS cells. The purpose of using hydrogels for T cell differentiation was to create more biomimetic reconstructions of the cell's natural surrounding within tissue that may help us one day better understand how to fine tune factors such as cell density, ligand density, and mechanical properties of the hydrogel in order to promote cell growth and differentiation. In terms of drug delivery, hydrogels offer targeted, site-specific, controlled release of therapeutic agents. The goal was to use the hydrophilic nature, stealth properties, and MADE chemistry of PEG to create enzyme-responsive drug carriers that can be inhaled and maintain presence in the deep lung until degraded to release biologic drugs.

In Chapter 2, the microgel system was introduced and the formulation of the system into a dry powder to be administered by DPI was explained. The freeze drying process utilized on the microgel system was confirmed as suitable and the swelling, degradation, and release kinetics of the microgels were determined to be acceptable and withstood the lyophilization process. The formulation part of the project, involved utilizing cryoprotectants and testing the dry powders for aerosolization properties. It was determined that the cryoprotectants were necessary to achieve aerodynamic diameter below 5 µm, necessary for pulmonary delivery. Lyophilizing microgels with InhaLac and blending the powder, allowed the powders to produce MMAD values between 1 µm and 3 µm and fine particles fractions of greater than 7%. The fine particle fraction was significantly increased when microgels were lyophilized with mannitol, however aerodynamic diameters were not within the desired range. *In vivo* studies confirmed the

ability to deliver the microgels via intratracheal administration to mice and their presence was retained within the lungs after 2 weeks.

Future work must be done to further pinpoint the ideal formulation of the microgels for DPI. Thus far, we have found a suitable formulation with InhaLac and blending but more work can be done to increase the FPF. Also *in vivo* studies must be repeated to fully understand the results of the tissue homogenization obtained this experiment and why the fluorescent signal of microgels increased over time in the lungs. Once a dry powder formulation is chosen as the ideal formulation for delivery of the microgels, an *in vivo* experiment must be performed using DPI. Also further *in vitro* studies with avoidance of alveolar macrophages must be performed. The formulation must also be tested with biologic drugs to test whether the cryroprotectant performs its duty in protecting the microcarrier as well as the drug from the stresses of the freeze drying process.

Chapter 3 successfully demonstrated the encapsulation of stem cells and stromal cells in the PEG based hydrogels and the ability of the hydrogels to act as microenvironments for the cells during early T cell differentiation. The cocultures of HSCs and OP9-DL1 cells were encapsulated within hydrogels were compared to 2D plated cocultures established in the literature. The hydrogels did not produce a higher or equivalent percentage of early T cells expressing Thy1.2 markers after 8 days than the 2D coculture. Still the population of Thy1.2 cells was present and correlated with the 2D population as expressing DN2 stage markers. The hydrogels in this experiment, although producing a smaller percentage of T cells, offer the advantage of not having to passage the cells every two to three days like the 2D cocultures require. Also, the hydrogel system offers more options in terms of cell density, hydrogel components, and mechanical properties that can be further fine-tuned in the future. Immobilized bDLL4 was

incorporated in the hydrogels as well. When compared to other bDLL4 approaches, the hydrogel performed very well and expressed a similar percentage of Thy1.2+ cells as the plated cultures with 2mg of bDLL4 with defined media and a more extensive cytokine cocktail. This is promising for the utilization of the gels for stromal free approaches in the differentiation of T cells.

Murine embryonic (R1) stem cells and induced pluripotent stem (iPS) cells were also encapsulated within the hydrogels with OP9-DL1 or bDLL4 coated beads. Co-encapsulation of R1 or iPS cells with OP9-DL1 cells or DLL4 microbeads in bulk hydrogels resulted in early T cell differentiation however were not an improvement from the 2D plated cocultures. Nonetheless, the hydrogels showed they are capable of early T cell differentiation with and without the presence of stromal cells which is a great advancement that should be further studied.

References

Abdelwahed, W., Degobert, G., Stainmesse, S., and Fessi, H. (2006a). Freeze-drying of nanoparticles: Formulation, process and storage considerations. 2006 Suppl. Non-Themat. Collect. 58, 1688–1713.

Abdelwahed, W., Degobert, G., and Fessi, H. (2006b). Investigation of nanocapsules stabilization by amorphous excipients during freeze-drying and storage. Eur. J. Pharm. Biopharm. 63, 87–94.

Ahsan, F., Rivas, I.P., Khan, M.A., and Torres Suárez, A.I. (2002). Targeting to macrophages: role of physicochemical properties of particulate carriers—liposomes and microspheres—on the phagocytosis by macrophages. J. Controlled Release 79, 29–40.

Anderson, G., and Takahama, Y. (2012). Thymic epithelial cells: working class heroes for T cell development and repertoire selection. Spec. Focus Struct. Funct. Lymphoid Tissues 33, 256–263.

Beckstead, B.L., Santosa, D.M., and Giachelli, C.M. (2006). Mimicking cell–cell interactions at the biomaterial–cell interface for control of stem cell differentiation. J. Biomed. Mater. Res. A 79A, 94–103.

Berrih, S. (1985). Extracellular matrix of the human thymus: immunofluorescence studies on frozen sections and cultured epithelial cells. J. Histochem. Cytochem. 33, 655–664.

Bhavsar, M., and Amiji, M. (2008). Development of Novel Biodegradable Polymeric Nanoparticles-in-Microsphere Formulation for Local Plasmid DNA Delivery in the Gastrointestinal Tract. AAPS PharmSciTech 9, 288–294.

Brannon-Peppas, L. (1990). Preparation and Characterization of Crosslinked Hydrophilic Networks. In Studies in Polymer Science, Lisa Brannon-Peppas and Ronald S. Harland, ed. (Elsevier), pp. 45–66.

Carlson, M.E. (2007). Notch signaling pathway and tissue engineering. Front. Biosci. 12, 5143–5156.

Cha, C., Liechty, W.B., Khademhosseini, A., and Peppas, N.A. (2012). Designing Biomaterials To Direct Stem Cell Fate. ACS Nano 6, 9353–9358.

Cho, S.K., Webber, T.D., Carlyle, J.R., Nakano, T., Lewis, S.M., and Zúñiga-Pflücker, J.C. (1999). Functional Characterization of B Lymphocytes Generated in vitro from Embryonic Stem Cells. Proc. Natl. Acad. Sci. U. S. A. 96, 9797–9802.

Ciofani, M., and Zúñiga-Pflücker, J.C. (2007). The Thymus as an Inductive Site for T Lymphopoiesis. Annu. Rev. Cell Dev. Biol. 23, 463–493.

Daley, G.Q. (2003). Realistic prospects for stem cell therapeutics. Hematology 398–418.

DALEY, G.Q. (2003). From Embryos to Embryoid Bodies. Ann. N. Y. Acad. Sci. 996, 122–131.

Dallas, M.H., Varnum-Finney, B., Delaney, C., Kato, K., and Bernstein, I.D. (2005). Density of the Notch ligand Delta1 determines generation of B and T cell precursors from hematopoietic stem cells. J. Exp. Med. 201, 1361–1366.

Dudley, M.E., and Rosenberg, S.A. (2003). Adoptive-cell-transfer therapy for the treatment of patients with cancer. Nat Rev Cancer 3, 666–675.

Edwards, D.A., and Dunbar, C. (2002). BIOENGINEERING OF THERAPEUTIC AEROSOLS. Annu. Rev. Biomed. Eng. 4, 93–107.

Ehrbar, M., Rizzi, S.C., Schoenmakers, R.G., San Miguel, B., Hubbell, J.A., Weber, F.E., and Lutolf, M.P. (2007). Biomolecular Hydrogels Formed and Degraded via Site-Specific Enzymatic Reactions. Biomacromolecules 8, 3000–3007.

El-Sherbiny, I.M., McGill, S., and Smyth, H.D.C. (2010). Swellable microparticles as carriers for sustained pulmonary drug delivery. J. Pharm. Sci. 99, 2343–2356.

Engler, A.J., Sen, S., Sweeney, H.L., and Discher, D.E. (2006). Matrix Elasticity Directs Stem Cell Lineage Specification. Cell 126, 677–689.

Evora, C., Soriano, I., Rogers, R.A., Shakesheff, K.M., Hanes, J., and Langer, R. (1998). Relating the phagocytosis of microparticles by alveolar macrophages to surface chemistry: the effect of 1,2-dipalmitoylphosphatidylcholine. J. Controlled Release 51, 143–152.

Fleige, E., Quadir, M.A., and Haag, R. (2012). Stimuli-responsive polymeric nanocarriers for the controlled transport of active compounds: Concepts and applications. Approaches Drug Deliv. Based Princ. Supramol. Chem. 64, 866–884.

Fraser, J.R.E., Laurent, T.C., and Laurent, U.B.G. (1997). Hyaluronan: its nature, distribution, functions and turnover. J. Intern. Med. 242, 27–33.

Germain, R.N. (2002). T-cell development and the CD4-CD8 lineage decision. Nat Rev Immunol 2, 309–322.

Ghosh, K., Pan, Z., Guan, E., Ge, S., Liu, Y., Nakamura, T., Ren, X.-D., Rafailovich, M., and Clark, R.A.F. (2007). Cell adaptation to a physiologically relevant ECM mimic with different viscoelastic properties. Biomaterials 28, 671–679.

Gravano, D.M., and Manilay, J.O. (2010). Inhibition of proteolysis of Delta-like-1 does not promote or reduce T-cell developmental potential. Immunol. Cell Biol. 88, 746–753.

Haylock, D.N., and Nilsson, S.K. (2006). The role of hyaluronic acid in hemopoietic stem cell biology. Regen. Med. 1, 437+.

Hirose, K., Marui, A., Arai, Y., Kushibiki, T., Kimura, Y., Sakaguchi, H., Yuang, H., Chandra, B.I.R.S., Ikeda, T., Amano, S., et al. (2008). Novel approach with intratracheal administration of microgelatin hydrogel microspheres incorporating basic fibroblast growth factor for rescue of rats with monocrotaline-induced pulmonary hypertension. J. Thorac. Cardiovasc. Surg. 136, 1250–1256.

Holst, J., Watson, S., Lord, M.S., Eamegdool, S.S., Bax, D.V., Nivison-Smith, L.B., Kondyurin, A., Ma, L., Oberhauser, A.F., Weiss, A.S., et al. (2010). Substrate elasticity provides mechanical signals for the expansion of hemopoietic stem and progenitor cells. Nat Biotech 28, 1123–1128.

Hozumi, K., Mailhos, C., Negishi, N., Hirano, K., Yahata, T., Ando, K., Zuklys, S., Holländer, G.A., Shima, D.T., and Habu, S. (2008). Delta-like 4 is indispensable in thymic environment specific for T cell development. J. Exp. Med. 205, 2507–2513.

Irngartinger, M., Camuglia, V., Damm, M., Goede, J., and Frijlink, H.. (2004). Pulmonary delivery of therapeutic peptides via dry powder inhalation: effects of micronisation and manufacturing. Eur. J. Pharm. Biopharm. 58, 7–14.

Izon, D.J., Punt, J.A., and Pear, W.S. (2002). Deciphering the role of Notch signaling in lymphopoiesis. Curr. Opin. Immunol. 14, 192–199.

Jenkinson, E.J., and Anderson, G. (1994). Fetal thymic organ cultures. Curr. Opin. Immunol. 6, 293–297.

Koch, U., Fiorini, E., Benedito, R., Besseyrias, V., Schuster-Gossler, K., Pierres, M., Manley, N.R., Duarte, A., MacDonald, H.R., and Radtke, F. (2008). Delta-like 4 is the essential, nonredundant ligand for Notch1 during thymic T cell lineage commitment. J. Exp. Med. 205, 2515–2523.

Konan, Y.N., Gurny, R., and Allémann, E. (2002). Preparation and characterization of sterile and freeze-dried sub-200 nm nanoparticles. Int. J. Pharm. 233, 239–252.

Laky, K., Fleischacker, C., and Fowlkes, B.J. (2006). TCR and Notch signaling in CD4 and CD8 T-cell development. Immunol. Rev. 209, 274–283.

Lee, J., and Kotov, N.A. (2009). Notch Ligand Presenting Acellular 3D Microenvironments for ex vivo Human Hematopoietic Stem-Cell Culture made by Layer-By-Layer Assembly. Small 5, 1008–1013.

Lee, K.Y., and Mooney, D.J. (2001). Hydrogels for Tissue Engineering. Chem. Rev. 101, 1869–1880.

Lehar, S.M., and Bevan, M.J. (2002). T Cell Development in Culture. Immunity 17, 689–692.

Lin, C.-C., and Metters, A.T. (2006). Hydrogels in controlled release formulations: Network design and mathematical modeling. Comput. Drug Deliv. 58, 1379–1408.

Lutolf, M.P., and Hubbell, J.A. (2003). Synthesis and Physicochemical Characterization of End-Linked Poly(ethylene glycol)-co-peptide Hydrogels Formed by Michael-Type Addition. Biomacromolecules 4, 713–722.

Lutolf, M.P., Gilbert, P.M., and Blau, H.M. (2009a). Designing materials to direct stem-cell fate. Nature 462, 433–441.

Lutolf, M.P., Doyonnas, R., Havenstrite, K., Koleckar, K., and Blau, H.M. (2009b). Perturbation of single hematopoietic stem cell fates in artificial niches. Integr. Biol. 1, 59–69.

Miller, J.S. (2005). Successful adoptive transfer and in vivo expansion of human haploidentical NK cells in patients with cancer. Blood 105, 3051–3057.

Mohtashami, M., Shah, D.K., Nakase, H., Kianizad, K., Petrie, H.T., and Zúñiga-Pflücker, J.C. (2010). Direct Comparison of Dll1- and Dll4-Mediated Notch Activation Levels Shows Differential Lymphomyeloid Lineage Commitment Outcomes. J. Immunol. 185, 867–876.

La Motte-Mohs, R.N. (2005). Induction of T-cell development from human cord blood hematopoietic stem cells by Delta-like 1 in vitro. Blood 105, 1431–1439.

Nakano, T., Kodama, H., and Honjo, T. (1994). Generation of Lymphohematopoietic Cells from Embryonic Stem Cells in Culture. Science 265, 1098–1101.

O'Connor, R.S. (2012). Substrate rigidity regulates human T cell activation and proliferation. J. Immunol. 1950 189, 1330–1339.

Patel, B., Gupta, V., and Ahsan, F. (2012). PEG–PLGA based large porous particles for pulmonary delivery of a highly soluble drug, low molecular weight heparin. J. Controlled Release 162, 310–320.

Peppas, N.A., Keys, K.B., Torres-Lugo, M., and Lowman, A.M. (1999). Poly(ethylene glycol)-containing hydrogels in drug delivery. J. Controlled Release 62, 81–87.

Peppas, N.A., Bures, P., Leobandung, W., and Ichikawa, H. (2000). Hydrogels in pharmaceutical formulations. Eur. J. Pharm. Biopharm. 50, 27–46.

Peppas, N.A., Slaughter, B.V., and Kanzelberger, M.A. (2012). 9.20 - Hydrogels. In Polymer Science: A Comprehensive Reference, Editors-in-Chief: Krzysztof Matyjaszewski, and Martin Möller, eds. (Amsterdam: Elsevier), pp. 385–395.

Pilcer, G., and Amighi, K. (2010). Formulation strategy and use of excipients in pulmonary drug delivery. Int. J. Pharm. 392, 1–19.

Plautz, G.E., Bukowski, R.M., Novick, A.C., Klein, E.A., Kursh, E.D., Olencki, T.E., Yetman, R.J., Pienkny, A., Sandstrom, K., and Shu, S. (1999). T-cell adoptive immunotherapy of metastatic renal cell carcinoma. Urology 54, 617–623.

Preiss, M.R. (2011). Stimuli-responsive liposome-nanoparticle assemblies. Expert Opin. Drug Deliv. 8, 1025–1040.

Prestwich, G.D. (2011). Hyaluronic acid-based clinical biomaterials derived for cell and molecule delivery in regenerative medicine. Proc. Fifthteenth Int. Symp. Recent Adv. Drug Deliv. Syst. 155, 193–199.

Pui, J.C., Allman, D., Xu, L., DeRocco, S., Karnell, F.G., Bakkour, S., Lee, J.Y., Kadesch, T., Hardy, R.R., Aster, J.C., et al. (1999). Notch1 Expression in Early Lymphopoiesis Influences B versus T Lineage Determination. Immunity 11, 299–308.

Pusztai, A. (1997). Both free and complexed trypsin inhibitors stimulate pancreatic secretion and change duodenal enzyme levels. Am. J. Physiol. 272, G340–50.

Radtke, F., Wilson, A., Stark, G., Bauer, M., van Meerwijk, J., MacDonald, H.R., and Aguet, M. (1999). Deficient T Cell Fate Specification in Mice with an Induced Inactivation of Notch1. Immunity 10, 547–558.

Rosenberg, S.A., and Dudley, M.E. (2009). Adoptive cell therapy for the treatment of patients with metastatic melanoma. Lymph. Dev. Tumour Immunol. Ed. Casey Weav. Alexander Rudensky Ton Schumacher Nick Restifo 21, 233–240.

Saez, A., Guzmán, M., Molpeceres, J., and Aberturas, M.. (2000). Freeze-drying of polycaprolactone and poly(d,l-lactic-glycolic) nanoparticles induce minor particle size changes affecting the oral pharmacokinetics of loaded drugs. Eur. J. Pharm. Biopharm. 50, 379–387.

Schmitt, T.M., and Zúñiga-Pflücker, J.C. (2002). Induction of T Cell Development from Hematopoietic Progenitor Cells by Delta-like-1 In Vitro. Immunity 17, 749–756.

Schmitt, T.M., and Zúñiga-Pflücker, J.C. (2006). T-cell development, doing it in a dish. Immunol. Rev. 209, 95–102.

Schmitt, T.M., de Pooter, R.F., Gronski, M.A., Cho, S.K., Ohashi, P.S., and Zuniga-Pflucker, J.C. (2004). Induction of T cell development and establishment of T cell competence from embryonic stem cells differentiated in vitro. Nat Immunol 5, 410–417.

Schwarz, C., and Mehnert, W. (1997). Freeze-drying of drug-free and drug-loaded solid lipid nanoparticles (SLN). Int. J. Pharm. 157, 171–179.

Sharon Gerecht, Jason A. Burdick, Ferreira, L.S., Townsend, S.A., Langer, R., and Vunjak-Novakovic, G. (2007). Hyaluronic Acid Hydrogel for Controlled Self-Renewal and Differentiation of Human Embryonic Stem Cells. Proc. Natl. Acad. Sci. U. S. A. 104, 11298–11303.

Shu, X.Z., Liu, Y., Palumbo, F., and Prestwich, G.D. (2003). Disulfide-crosslinked hyaluronan-gelatin hydrogel films: a covalent mimic of the extracellular matrix for in vitro cell growth. Biomaterials 24, 3825–3834.

De Smedt, M., Hoebeke, I., and Plum, J. (2004). Human bone marrow CD34+ progenitor cells mature to T cells on OP9-DL1 stromal cell line without thymus microenvironment. Work. Haploidentical Hematop. Stem Cell Transplant. 33, 227–232.

Stegemann, S., Kopp, S., Borchard, G., Shah, V.P., Senel, S., Dubey, R., Urbanetz, N., Cittero, M., Schoubben, A., Hippchen, C., et al. (2013). Developing and advancing dry powder inhalation towards enhanced therapeutics. Eur. J. Pharm. Sci. 48, 181–194.

Tammi, M.I. (2002). Hyaluronan and homeostasis: a balancing act. J. Biol. Chem. 277, 4581–4584.

Taqvi, S., Dixit, L., and Roy, K. (2006). Biomaterial-based notch signaling for the differentiation of hematopoietic stem cells into T cells. J. Biomed. Mater. Res. A 79A, 689–697.

Varnum-Finney, B. (2000). Immobilization of Notch ligand, Delta-1, is required for induction of notch signaling. J. Cell Sci. 113 Pt 23, 4313–4318.

Varnum-Finney, B. (2003). Combined effects of Notch signaling and cytokines induce a multiple log increase in precursors with lymphoid and myeloid reconstituting ability. Blood 101, 1784–1789.

Wanakule, P., Liu, G.W., Fleury, A.T., and Roy, K. (2012). Nano-inside-micro: Disease-responsive microgels with encapsulated nanoparticles for intracellular drug delivery to the deep lung. J. Controlled Release 162, 429–437.

Yee, C. (2006). Adoptive T-Cell Therapy of Cancer. Immunother. Cancer 20, 711–733.

Zhang, J., Skardal, A., and Prestwich, G.D. (2008). Engineered extracellular matrices with cleavable crosslinkers for cell expansion and easy cell recovery. Biomaterials 29, 4521–4531.

Zheng Shu, X., Liu, Y., Palumbo, F.S., Luo, Y., and Prestwich, G.D. (2004). In situ crosslinkable hyaluronan hydrogels for tissue engineering. Biomaterials 25, 1339–1348.

Zuniga-Pflucker, J.C. (2004). T-cell development made simple. Nat Rev Immunol 4, 67–72.

Vita

Asha Fleury obtained a Bachelor's degree in Biomedical Engineering at the University of Texas at Austin in 2010. During her undergraduate years, she worked as a research assistant in the Laboratory of Biomaterials, Drug Delivery and Bionanotechnology where she conducted research with intelligent hydrogels for oral protein delivery under the supervision of Dr. Nicholas Peppas. She also obtained experience in the field of neural tissue engineering as a research assistant at the Iowa State University in the laboratory of Dr. Surya Mallapragada. Asha continued her education by pursuing graduate studies at the University of Texas at Austin, where she studied hydrogel applications in pulmonary drug delivery and biomaterial systems for *in vitro* T cell differentiation in the Laboratory for Cellular and Macromolecular Engineering under the supervision of Dr. Krishnendu Roy. She also balanced her research with pursuits in educational activities for young students, mentoring undergraduates, and endeavors into the field of technology and public policy.

Permanent email: fleury@utexas.edu

This thesis was typed by Asha Tarika Fleury.